Trends in Arctic Aerosol Sources, Chemical Composition, and Optical Properties at Utqiaġvik, Alaska

_____

A THESIS

Presented to

The Faculty of the Environmental Studies Department

at Colorado College

In Partial Fulfillment of the Requirements for the Degree

Bachelor of Arts

By

Allison Moon

May 2021

Trends in Arctic Aerosol Sources, Chemical Composition, and Optical Properties at Utqiaġvik, Alaska

Allison Moon

May 2021

Environmental Science

Abstract

Arctic haze is the seasonal maximum of atmospheric aerosols in the Arctic that occurs every year in the late winter and early spring. Chemical components of Arctic haze include particulate matter from air pollution, dust, organic matter, and sea salt. Air pollution transported from lower latitudes dictates ice-albedo and cloud radiation feedbacks, which contribute to either accelerated or abated warming in the Arctic. Consequently, understanding the sources, transport, and composition of aerosols in the Arctic is imperative. Researchers at Barrow Atmospheric Baseline Observatory (BRW), now affiliated with The National Oceanic and Atmospheric Administration (NOAA), have been measuring atmospheric chemical composition at Utqiaġvik, Alaska since 1976. Large volumes of air are filtered through size-segregated filters at BRW over 1 to 5-day timescales for submicron particles (particle diameter<1μm) and one-week to one-month timescales for supermicron particles (1μm<particle diameter<10μm). The filters are weighed, extracted, and then characterized via ion chromatography. The Hybrid Single-Particle Lagrangian Integrated Trajectory (HYSPLIT) model was used to evaluate trends in local and long-range transport of aerosols from 1997 to 2020. This study considers the sources and seasonality of aerosols at Utqiaġvik from 1998 to 2013 and determines their correspondence with processes within and outside the Arctic. Aerosol scattering and absorption at 550nm measured between 1998-2019 were used to assess linkages between optical properties and aerosol chemical composition. Findings reveal significant decreases in haze season non-sea salt sulfate, nitrate, and aerosol scattering at 550nm. These results suggest decreased aerosol acidity and wintertime changes in aerosol composition that may contribute to accelerated warming in the Arctic through direct radiative forcing and their impact on cloud nucleation processes. Trends in aerosol composition in summer at Utqiaġviksuggest enhanced biogenic non-sea salt sulfate production and long-range transport of absorbing species from biomass burning at lower latitudes, but more years of measurements are needed to demonstrate statistical significance. These results affirm the complex relationship between aerosol composition and radiative properties of the atmosphere, which is the current greatest uncertainty in global climate modeling (IPCC 2013).

Acknowledgments

I would like to express my sincere gratitude to Dr. Trish Quinn and Dr. Lynne Gratz for their insightful comments and suggestions and unwavering support. I am incredibly lucky to have these kind and brilliant women as mentors and this thesis would not have been possible without their guidance.

I am also grateful to the atmospheric chemistry research group at PMEL: Trish Quinn, Lucia Upchurch, Derek Coffman, Jim Johnson, and Timothy Bates for their contributions to this project and invaluable guidance during my research internship. Thanks also to Betsy Andrews in NOAA's Earth Systems Research Laboratory's (ESRL) Aerosol Group for helping gather and verify data for this project.

I would also like to thank the Colorado College Environmental Studies and Chemistry Programs and to acknowledge the professors at Colorado College who have encouraged and supported me throughout my undergraduate education, especially Dr. Lynne Gratz, Dr. Lina Basal, Dr. Ulyana Horodyskyj, Dr. Murphy Brasuel, and my advisor Dr. Marion Hourdequin. Thanks to Mindi May at Colorado Parks and Wildlife for her formative mentorship in high school and for inspiring me to pursue environmental science in college.

Thank you to my parents Naomi and Dave Moon and my sister Emma Moon for their unconditional love and for cheering me on in every endeavor, and my grandfathers Marvin Abraham and Ralph Moon for sparking my love for science at an early age and showing me the value of a public-service oriented career in research.

This research was supported by NOAA's Hollings Scholarship Program and Pacific Marine Environmental Laboratory. Thank you to the Barrow Baseline Observatory personnel over the years for their data collection for this project.

I would like to honor the Iñupiat people of Utqiaġvik, on whose homelands the Barrow Atmospheric Baseline Observatory sits. The Iñupiat people have lived in this region for 1,500 years in one of the oldest permanent settlements in the United States. Most scientific literature refers to this location as Barrow, Alaska; however, respecting the name Utqiaġvik is integral to decolonization and for preserving the Inupiaq ancestral language.

Table of Contents

I. Introduction:

In the late 1800s, scientists and explorers drawn to the high Arctic were mystified by the seasonal atmospheric phenomenon that is now known as Arctic haze (Daubrée 1874, Garrett and Verzella 2008). Records from the First International Polar Year expedition, which was held 1882-1883 at Point Barrow, Alaska, described periods of haze in Arctic winter and early spring (Taylor 1981). In a 1906 lecture, George C. Simpson put his and his colleagues' bewilderment into words:

> "All who have traveled in Arctic regions know the peculiar haze which fills the air when the temperature falls very low and gives the 'cold' aspect to Arctic scenes. Such a haze, which is not a mist or fog, was frequent during the winter in Karasjok [69°N in Norway]. On the other hand, at the end of the summer, the air reached a degree of transparency which I have never seen equaled in any other place (Garrett and Verzella 2008)".

Nearly a century later, in 1976, Glenn Shaw from the University of Alaska at Fairbanks began observing atmospheric aerosols at Barrow Atmospheric Baseline Observatory (BRW) by measuring their light-scattering properties and particle number concentrations (Shaw 1982). Rigorous chemical analysis performed by Glenn Shaw and his colleagues at Utqiaġvikrevealed a clue for the cause of the mysterious haze phenomenon. High concentrations of vanadium were consistent with substantial amounts of heavy oil combustion and plumes of soil dust sourced from the Gobi Desert (Shaw 1982, Garrett and Verzella 2008). Thus, the unusual fluxes of aerosols were not coming from local sources, but the result of long-range transport of air pollution from lower latitudes (Shaw 1982).

Arctic haze is the seasonal maximum in atmospheric aerosols in the winter and early spring. Previous studies have revealed the cause of this atmospheric phenomenon: the increased particle concentrations are because of more efficient transport of pollutants from lower latitudes in Arctic winter compared to the summer (Quinn et al. 2002, Quinn et al. 2007, Shaw et al. 1982, Shaw et al. 1995). Also, increased atmospheric stability from strong temperature inversions acts as a lid that holds aerosols in place (Quinn et al. 2007). This atmospheric stability does not allow for turbulent mixing of tropospheric layers or wet deposition, which are important pollutant removal pathways (Shaw et al. 1995). This accumulation of aerosols is responsible for the Arctic haze phenomenon since aerosols efficiently scatter radiation at mid-visible solar wavelengths.

Aerosols influence radiative forcing due to both their direct scattering and absorption properties and their role as cloud condensation nuclei (Tomasi 2007, IPCC 2013). Direct aerosol optical properties are size-dependent: for mid-visible wavelengths (550nm), particles that are between 0.2-1μm are most efficient at scattering light (Quinn et al. 1996). Aerosols also affect radiative forcing indirectly since they serve as cloud condensation nuclei; clouds with higher aerosol particle concentrations have smaller liquid droplets that can reflect solar radiation and have a cooling effect on climate (Abbatt et al. 2006, IPCC 2013). Ice nucleation is a cloud formation mechanism that occurs with both homogeneous and heterogeneous processes to form mixed-phase cirrus clouds (Gettelman et al. 2012, IPCC 2013, Zhou et al. 2019). Homogeneous nucleation was originally thought to be dominant between these two processes and is better understood; it requires temperatures

lower than -38℃ and cloud supersaturation for liquid water to freeze without the presence of cloud condensation nuclei (IPCC 2013). More recent findings in ice-phase microphysical processes suggest that heterogeneous nucleation is a more favorable ice nucleation pathway (Abbatt et al. 2006, IPCC 2013). This cloud formation process involves selective nucleation onto small aerosol particles called ice nuclei (IC), which requires dryer and warmer conditions than homogeneous ice nucleation (Abott et al. 2006, Gettlemen et al. 2012, IPCC 2013). Aerosol impact on direct radiative forcing and cloud formation is contingent upon aerosol size distribution, chemical composition, hygroscopic properties, and mixing state (abbatt et al. 2006, Gettlemen et al. 2012, Fisher et al. 2011, IPCC 2013). Thus, understanding long-term trends in chemical composition and optical properties of aerosols is important for anticipating aerosol effects on climate at Utqiaġvik.

Particulate organic matter (POM), sulfate, and sea salt aerosol are principal components of Arctic haze while ammonium, nitrate, black carbon, crustal elements, and trace metals are minor components (AMAP 2006, IPCC 2013, Quinn et al. 2002). This study is centered around important inorganic aerosol species including non-sea salt sulfate, ammonium, nitrate, sodium, and chloride. Non-sea salt sulfate (nss $SO_4^{=}$) forms at lower latitudes from fossil fuel combustion and sulfide ore smelting and undergoes transport to the Arctic (Barrie et al. 1984, Hidy et al. 2016, Quinn et al. 2002, Stohl 2006). Additionally, sulfur dioxide (SO_2) transported from Europe and Asia is photo-oxidized to form non-sea salt sulfate in the Arctic (Barrie et al. 1984). Sulfur dioxide and sulfate aerosol can undergo long-range transport to the Arctic

across the Pacific from Asia and other developing countries in their short lifetimes of a few days to a week (Barrie et al. 1984, Hidy et al. 2016).

Ammonium (NH_4^+) concentrations are tied to sulfate aerosol since it forms when gas-phase ammonia (NH_3) reacts with sulfate aerosol to form ammonium sulfate ($(NH_4)_2SO_4$) and ammonium bisulfate ($(NH_4)HSO_4$) (Drugé et al. 2019, Fisher et al. 2011). Sources of ammonia include natural emissions from soil, vegetation, and the ocean (Quinn et al. 2008). Anthropogenic sources of ammonia come from fertilizer production and use, biomass burning, and waste from domestic animals (Quinn et al. 2002, Quinn et al. 2008). Ammonia (NH_3) reacts instantly and irreversibly with sulfuric acid (H_2SO_4) aerosol due to its low vapor pressure (Drugé et al. 2019). The product of this reaction, ammonium sulfate, neutralizes the strong acid and decreases its ability to attract and retain water molecules (Fisher et al. 2011). The hygroscopicity reduction attenuates aerosol scattering and affects ice-nucleation processes, which can lead to enhanced warming (Fisher et al. 2011).

Nitrate aerosol (NO_3^-), another species associated with ammonium formation, is derived from NO_x species that originate from natural and anthropogenic processes at lower latitudes. Sources include industrial emissions and oil and gas activity, especially from Europe and Asia (AMAP 2006, Law and Stohl 2007). Nitrogen species are emitted naturally from volcanic activity, boreal forest fires, and from snowpack via photolysis (Law and Stohl 2007). Nitrate aerosol contributes to aerosol acidity, though not as much as sulfate in the Arctic (AMAP 2006). Excess NH_3 that does not react with nss $SO_4^=$ aerosol neutralizes nitric acid (HNO_3) to form ammonium nitrate (NH_4NO_3) (Drugé et al. 2019, Hara et al. 1999).

This reaction reduces the correlation between ammonium: sulfate species and the acidity of aerosol composition. Since nitrate formation is a heterogeneous process that is dependent on particle size, ammonia and sulfate concentrations, relative humidity, and temperature, there is more uncertainty in modeling NO_3^- concentrations and radiative forcing. However, nitrate has known scattering, hygroscopic, and cloud nucleation properties (Bauer et al. 2007, Boucher et al. 2013, Hand et al. 2007, IPCC 2013).

Arctic fractionation of nitrogen species is also tied to heterogeneous reactions on supermicron sea salt particles, the primary mechanism for NO_3^- formation in Arctic winter (Hara et al. 1999, Hara et al. 2002, McInnes et al. 1994). Sea salt particles have a liquid surface where reactive nitrogen species including HNO_3, N_2O_5, and NO_3 enter the aqueous phase resulting in particulate NO_3^- aerosol formation and chloride depletion (Hara et al. 1999). Besides its important role in nitrogen species partitioning, sea salt aerosol is a major contributor to aerosol particle mass and scattering properties (Quinn et al. 2002). Several mechanisms introduce sea salt aerosol into the atmosphere: in the winter, blowing snow and frost flowers loft submicron sea salt into the atmosphere at Utqiaġvik (Jacobi et al. 2009, Jacobi et al. 2012). In summer, supermicron sea salt particles enter the atmosphere via wind-driven processes on the ocean's surface (Quinn et al. 2002, Quinn et al. 2016). Sea salt aerosol is an important component of aerosol particle mass composition and serves as an indicator of aerosol acidity by measuring chloride depletion of sea salt particles (Quinn et al. 2002).

Understanding the physical and chemical properties of atmospheric aerosols is imperative for climate sensitivity modeling in the Arctic (Boucher et al. 2013, Yin et al. 2014). In this study, seasonal trends in chemical composition (1998-2013) and optical properties (1998-2019) of aerosols at Utqiaġvik, AK are quantified to assess how these trends correspond to processes within and outside the Arctic.

II. Methods

2.1 Sample collection and chemical analysis

Aerosol samples are collected at Barrow Atmospheric Baseline Observatory (BRW) with an automated filter sampling system. Sample air enters the stack 10m above ground level into a 4.45 cm inner diameter stainless steel tube. Real-time wind speed and direction measurements at the top of the 10m tall sample inlet are used to prevent contamination from local pollution from Utquiagvik. Sample air is pulled through the filters only when winds are from the "clean sector" of 0 to 130 degrees (Quinn et al. 2002). A flow rate of 1000 L/min is split into a sample flow of 150 L/min and a sheath flow of 850 L/min (Delene and Ogren 2002). Samples are then directed into 1.6 cm inner diameter flow lines at a flow rate of 30 L/min.

A Berner-type multijet cascade impactor is used to segregate sampled aerosol into two size ranges — submicron particles (particle diameter < 1 μm) and supermicron particles (1 μm < particle diameter < 10 μm) (Berner 1979). Large particles can bounce onto downstream stages of the impactor. The artifact is minimized by applying silicone on a grease cup above the 10 μm impactor stage and spraying the 1 and 10 μm sampling substrates with silicon (Quinn et al. 2002).

Computer-controlled solenoid valves automatically open and close to collect aerosol samples. Submicron particles are collected by a filter carousel with 8 Millipore Fluoropore filters. Sample duration for submicron samples ranges between 1 to 5 days according to time of year and aerosol loading. Since more aerosol loading occurs in the haze season, sampling times are 1-3 days in the haze

season and 4-5 days in the summer. Supermicron particles collected on a Tedlar film have longer sampling times than submicron species since there is only one Tedlar film sampled per 8 Millipore filters. Haze season supermicron sampling periods are between 6-7 days, and summer samples are collected over one month. Blanks are prepared by exposing a filter to ambient air for 10 seconds. All field samples are blank corrected by subtracting background concentrations detected on the blank filters.

Upon arrival at PMEL, impactor film and carousel filter handling are done in a glove box continually purged with air that is scrubbed with potassium carbonate and citric acid preventing contamination of the filters by acids and bases. Filters and films are wetted with 1mL of spectral grade methanol and 5mL of distilled deionized water. Substrates in the methanol-water solution are extracted with sonication for 30 minutes. Ion chromatography is used to measure concentrations of major ionic species. Cations measured include Ca^{2+}, K^{+}, Mg^{2+}, Na^{+}, and NH_4^{+}. Anions measured include Cl^{-}, MSA^{-} (methanesulfonate), NO_3^{-}, and $SO_4^{=}$. (Quinn 1982).

IC results are quality controlled with statistical analysis and sample volume consideration. Since sample concentrations are calculated by dividing the total volume of air drawn through a filter sample, samples with low volumes sometimes yield high concentrations that are not representative of atmospheric conditions. Samples with concentrations two standard deviations higher than the seasonal mean are evaluated for low volume errors. Samples with volumes less than 10 m^2 that show statistically influential values for multiple species are omitted from the calculated seasonal averages.

Sodium is a tracer species for sea salt aerosol and is used to calculate non-sea salt concentrations of calcium, potassium, magnesium, and sulfate aerosol (Holland 1978). Non-sea salt concentrations are calculated for calcium, potassium, magnesium, and sulfate by subtracting the expected mass ratio of the species with sodium in seawater from the total measured concentration of that species. For sulfate, non-sea salt concentrations are calculated with the equation nss $SO_4^{=}$ = total $SO_4^{=}$] - (0.252 × [Na^+]). The seawater mass ratio for calcium to sodium is 0.0383, potassium to sodium is 0.0371, magnesium to sodium is 0.0120, and sulfate to sodium is 0.252 (Holland 1978).

2.2 Numerical Methods for Statistical Analysis

Trends in atmospheric transport, chemical composition, and optical properties at Utqiaġvik are analyzed using the MAKESENS model from the Finnish Meteorological Institute, which incorporates the Mann-Kendall test and Sen's slope estimates. The Mann-Kendall test and the nonparametric Sen's method are used to detect monatomic trends in time series of seasonal values (Salmi et al. 2002). Data are first separated by season: haze season is from January-April and summer is defined as July-September. Annual averages are calculated for each season and entered into the MAKESENS model.

The Mann-Kendall test is in the form $x = f(t) + \varepsilon$, where f(t) is the trend as a function of time and ε represents the residuals. Residuals are assumed to be from the same distribution, so the variance is assumed to be constant over time (Salmi et al. 2002). The Mann-Kendall test determines trend significance with a normal

approximation (Z-statistic) and S statistics for data sets that are longer than ten years. Statistically significant trends are evaluated using the Z-statistics for four levels of significance ($\propto$). The statistically significant results can have $\propto$-values of 0.001, 0.01, 0.05, and 0.1 with 0.1 reporting 90% significance and 0.001 reporting 99.9% significance (Salmi et al. 2002).

While the Mann-Kendall test detects statistically significant trends in the data, Sen's method estimates the slope of a linear trend (Salmi et al. 2002). The model is of the form f(t) = Qt + B where Q is the approximated slope and B is a constant. While this resembles a simple linear equation, the calculations for estimating Q involve estimating the rate of change between all data pairs, determining the median value, and computing a two-sided confidence interval for the approximation. The confidence interval is evaluated at $\propto$-values of 0.05 and 0.001 and incorporates the Z-statistic from the standard normal distribution and the variance of the data set (S) (Salmi et al. 2002). The confidence interval is of the form $C_\alpha = Z_{1-\alpha/2} \sqrt{(VAR(S))}$ where VAR(S) is the variance and $Z_{1-\alpha/2}$ is obtained from the normal distribution. These numerical methods were used to evaluate changes in atmospheric transport, aerosol composition, and optical properties at Utqiaġvik.

2.3 Atmospheric backtrajectories and NOAA HYSPLIT model

NOAA's Hybrid Single-Particle Lagrangian Integrated Trajectory (HYSPLIT) model shows the dominant sectors for atmospheric transport to Utqiaġvik (Roland et al. 1998, Quinn et al. 2002). The HYSPLIT model computes simple air parcel backtrajectories for a specific geographic location and time. GPS coordinates for

Barrow Atmospheric Baseline Observatory (71.2906° N, -156.7886° W) are the starting coordinates in the model.

Archived back trajectories are computed with the Global Data Assimilation System (GDAS). The GDAS system is utilized by the National Center for Environmental Prediction (NCEP) and uses a gridded three-dimensional model space to develop meteorological forecasts. The GDAS model incorporates surface observations, balloon data, wind profiles, buoy observations, and satellite observations to describe meteorological conditions.

HYSPLIT trajectories are calculated for isentropic vertical motion in 12-hr increments from 1997 to 2020 for run times of 168 hours (seven days) back in time. Trajectories are separated by differentiating arrival heights of 10m, 100m, and 1000m at BRW. Regions for atmospheric transport are separated by longitude and grouped into five regions: North America, the Pacific, Russia and Asia, Europe, and the Atlantic (figure 1). The five sectors are further separated by latitude to assess if transport to Utqiaġvik was short-range (confined to the Arctic) or long-range transport (from southern latitudes).

Data output for each trajectory is separated by arrival height and signifies the fraction of time the trajectory spent in each of the five sectors. To analyze long-term trends in aerosol sources at Utqiaġvik, seasonal averages of the trajectory sector distributions are evaluated using the MAKESENS model.

Figure 1: ArcGIS Map denoting the five sectors for trajectory analysis. Sectors were defined using GPS coordinates of Tokyo Japan, Vimajarivi Finland, Galway Ireland, Alert Canada, and Bethel Alaska. Utqiaġvik is shown by the blue marker. Back trajectories are expressed as the fraction of time each trajectory spent in the five sectors.

2.4 Optical measurements

Seasonal averages of scattering and absorption coefficients at 550 nm are calculated and used to assess trends in aerosol optical properties. A TSI 3563 nephelometer at a relative humidity of 20-40% measures aerosol scattering at 550 nm (Delene and Ogren 2002). Two Berner-type impacters upstream separate aerosol particles by size. Submicron and supermicron impacter airflow alternate every 5 min. Measured values are corrected for angular non-idealities due to non-Lambertian response (Anderson and Ogren 1998). Values are reported at 0°C, 1013 mbar, and the sample RH. Error in scattering measurements could be due to noise, calibration, insufficient correction for angular nonidealities, and adjustment to STP (Anderson and Ogren 1998, Quinn et al. 2002). Aerosol fine fraction is calculated by dividing a sample's submicron scattering coefficient by the combined submicron and supermicron scattering coefficients.

A Particle Soot Absorption Photometer (PSAP) is used to measure aerosol absorption coefficients by monitoring the change in transmission through a filter. Measurements are size-segregated with two impactors upstream from the instrument. Values are reported at 550 nm, 0°C, 1013 mbar, RH of the sample and are corrected for scattering artifact, deposit spot size, PSAP flow rate, and the manufacturer's calibration (Bond et al. 1999, Quinn et al. 2002)). Scattering and absorption coefficients are averaged for the submicron filter sampling periods and reported between 1998 and 2019.

III. Results and discussion

3.1 Trends in aerosol composition at Utqiaġvik

Seasonal transport of non-sea salt sulfate, a principal component of Arctic haze, dominates aerosol composition at Utqiaġvik (nss $SO_4^=$). Annual patterns in nss $SO_4^=$ exhibit maximums in the haze season that taper off in summer, yielding the sawtooth-like time series in figure 2 (Quinn et al. 2002). Besides seasonal differences, long-term trend analysis for aerosol composition at Utqiaġvik from 1998 to 2013 shows significant decreases in non-sea salt sulfate for both particle sizes in the haze season. The trends for haze season submicron nss $SO_4^=$ (-2.9% decrease, 90% significance) and supermicron nss $SO_4^=$ (-12% decrease, 99% significance) (figure 3) likely correspond to changes in anthropogenic emissions from Europe and North America, as discussed in section 3.2.

While emissions from lower latitudes are the dominant source of nss $SO_4^=$ at Utqiaġvik during the haze season, local biogenic processes in the summer contribute more to nss $SO_4^=$ composition at Utqiaġvik (Quinn et al. 2002, Quinn et al. 2009). Non-sea salt sulfate at Utqiaġvik forms biogenically via oxidation of dimethyl sulfide (C_2H_5S) (DMS) into SO_2 and then $SO_4^=$ in the spring and summer season (Ferek et al. 1995, Quinn et al. 2002). Dimethylsulfoniopropionate (DMSP) is emitted from oceanic phytoplankton and enzymatically cleaved to form DMS (Wang et al. 2018). In the springtime, trapped DMS under sea ice is released and oxidized to form atmospheric methanesulfonic acid (CH_4O_3S) (MSA^-) and biogenic nss nss $SO_4^=$ (Ferek et al. 1995, Quinn et al. 2002, Sharma et al. 2012, wang et al. 2018). Phytoplankton

productivity and DMS release increase with higher influxes of solar radiation and increased sea surface temperatures (SSTs) in the summer months (Quinn et al. 2009, Sharma et al. 2012). Summer supermicron nss $SO_4^=$ may be increasing at Utqiaġvik (+9.7% increase), which suggests enhanced local biogenic formation since supermicron particles have shorter atmospheric lifetimes and long-range transport of aerosols is not as prominent in the summer. This is because the Arctic front shifts northward and it is more difficult for warm air from lower latitudes to overcome the barrier in the lower troposphere (Stohl et al. 2006, Yang et al. 2018).

Sharma et al. (2012) examined sea ice-atmosphere exchange of DMS and biogenic aerosol formation mechanisms for Alert, Utquiagvik, and Ny-Ålesund in Arctic spring and summer (Sharma et al. 2012). The study found that biogenic sulfur formation is being enhanced by DMS release from melting sea ice, prolonged melt season, and enhanced MSA^- concentrations as a function of increased sea surface temperatures (Sharma et al. 2012). While mechanisms for biogenic non-sea salt sulfate formation in the Arctic have been documented, uncertainty remains in subsequent effects on cloud formation and radiative forcing (Sharma et al. 2012, IPCC 2013). As the Arctic warms, sea ice cover recedes, and the Arctic melt season expands, biogenic nss $SO_4^=$ production is likely to be enhanced at Utqiaġvik, though more data is needed to demonstrate statistical significance (Wang et al. 2018).

The relationship between atmospheric chemical composition and its effect on the heat budget in the Arctic is complicated; however, interannual variations of aerosol loading at Utqiaġvik certainly affect cloud properties and radiative forcing (IPCC 2013, Yin et al. 2014). Since sulfate is a cooling aerosol, reduced

concentrations in atmospheric nss $SO_4^=$ in the haze season may have a net warming effect in the Arctic through the decrease in aerosol scattering, and increased nss sulfate in the summer may have a net cooling effect. Further work in tying SSTs, sea ice cover, aerosol composition, and optical properties is merited to evaluate how these processes affect radiative forcing at Utqiaġvik.

Submicron ammonium (NH_4^+) shows no significant changes in concentration in either season between 1998 and 2013 (figure 4). Ammonium is dependent on nss $SO_4^=$ since it forms when ammonia and acidic sulfur species react (Quinn et al. 2002, Fisher et al. 2011, Drugé et al. 2019). The relationship between NH_4^+ and nss $SO_4^=$ particles is important for aerosol optical properties, cloud nucleation processes, as well as ammonium, sulfate, and nitrate partitioning (Abbatt et al. 2006, Gettlemen et al. 2012, Fisher et al. 2011, Girard et al. 2005, Guo et al. 2016, IPCC 2013). Linear regressions of NH_4^+:nss $SO_4^=$ molar ratios show a moderate correlation between the two species with a weaker correlation between the species in the haze season (R^2=0.42, p-value<0.001) compared to the summer (R^2= 0.56, p-value<0.001) (figure 5). These relationships are consistent with the expected influence nss $SO_4^=$ has on NH_4^+ formation, and a relative decrease in the amount of nss $SO_4^=$ compared to NH_3 indicates that nss $SO_4^=$ neutralization is being enhanced.

Ammonium-induced neutralization of nss sulfate decreases aerosol particle hygroscopicity, which both reduces direct aerosol scattering and renders supersaturated homogeneous nucleation to be unfavorable (Abbatt et al. 2006, Gettlemen et al. 2012, Girard et al. 2005, Fisher et al. 2011, IPCC 2013). This is important because heterogeneous ice nucleation of ammonium sulfate forms cirrus

clouds with larger and fewer ice crystals than homogeneous nucleation, which decreases cloud surface albedo (Abbatt et al. 2006). Through these mechanisms, increased neutralization of non-sea salt sulfate is expected to induce a net warming effect through both direct radiative forcing and ice nucleation processes (Abbatt et al. 2006, Fisher et al. 2011, IPCC 2013).

Nitrate (NO_3^-), another marker for aerosol acidity, exhibits a similar seasonal cycle to nss $SO_4^=$ with maximum concentrations in the haze season. The time series in figure 6 and the sawtooth pattern observed in figure 7 show seasonal fluctuations of nitrate aerosol concentrations at Utqiaġvik. Though NO_3^- and nss $SO_4^=$ both show similar seasonal cycles over longer timescales, annual variability demonstrates that these two species both increase in concentration in the haze season but by different magnitudes (figure 8). Like nss $SO_4^=$ supermicron NO_3^- is decreasing in the haze season (figure 9). This trend was among the most significant changes in this study (-8.3% decrease, 99% significance) (figure 9). Differences in seasonal fluctuations of nss sulfate and nitrate are due to different pollutant sources and pH-dependent reactions that affect nitrate partitioning (Dennis et al. 2008, Guo et al. 2016, Quinn et al. 2008).

The complex relationship between ammonium, nitrate, and sulfate species is one of the greatest uncertainties in modeling aerosol composition (Dennis et al. 2008, Guo et al. 2016). Alert, another long-term monitoring site North of Utqiaġvik at 82.50°N, 62.35°W, has exhibited opposite NO_3^- trends compared to those observed at BRW since NO_3^- has increased by 20% since the 1990s (Quinn et al. 2007, Sharma et al. 2019). While results from a 2007 study comparing the field sites found NO_3^- to

be increasing at Alert, trends in NO_3^- concentrations were not statistically significant between 1997 to 2006 (Quinn et al. 2007). More than a decade later, Sharma et al. (2019) reported an increasing trend in NO_3^- at Alert, despite a 40% reduction in European and Asian emissions since 1990 (Sharma et al. 2019). This result is explained by an ammonia-dependent shift in nitrate partitioning, and the nonlinear relationship between ammonia, nitrate, and sulfur dioxide which dictates nitrate aerosol concentrations (Dennis 2008, Guo et al. 2016). The ratio of ammonia to sulfur compounds increased at Alert - this allowed for more ammonium nitrate (NH_4NO_3) formation by converting gaseous nitric acid (HNO_3) into nitrate aerosol (NO_3^-) (Drugé et al. 2019, Sharma et al. 2019).

At Utqiaġvik, trend analysis showed no significant changes in ammonium concentrations, so the ammonia-dependent shift to form nitrate is not happening at Utqiaġvik like it is at Alert (figure 4). Thus, nitrate and sulfate concentrations have decreased with reduced emissions from lower latitudes (figures 3 and 8). Weaker correlation for the haze season NH_4:nss $SO_4^=$ linear regression in figure 5 is explained by partitioning of NH_4^+, nss $SO_4^=$, and NO_3^- (Guo et al. 2016). Reduced emissions of sulfur compounds from lower latitudes have decreased ammonia uptake in ammonium sulfate formation, leaving excess ammonia for ammonium nitrate formation (Drugé et al. 2019). Also, haze season NO_3^- concentrations are higher than summer concentrations by one order of magnitude which makes ammonium nitrate formation more favorable than in the summer (figures 7 and 8) (Drugé et al. 2019). The ratio of ammonium to sulfate aerosol is not high enough to

result in nitrate enrichment like Alert, but it explains the weaker correlation between ammonium and sulfate in the haze season observed in figure 5.

Sulfur is considered the most important acidifying pollutant for terrestrial ecosystems due to high anthropogenic emissions of sulfur compounds and efficient atmospheric transport to the Arctic (AMAP 2006). Decreased haze season nss $SO_4^{=}$ and NO_3^- and unchanging NH_4^+ concentrations have likely resulted in greater neutralization of atmospheric aerosol. This is important because terrestrial, aquatic, and cryospheric ecosystems in the high Arctic are vulnerable to gaseous and aerosol contamination (Meijer et al. 2003, Wania et al. 2003, AMAP 2006). Research in the European Arctic documents direct impacts of sulfur dioxide uptake in terrestrial vegetation, though it is believed that most of the Arctic vegetation is not threatened by air pollution from lower latitudes (AMAP 2006). However, freshwater systems are more susceptible to pollution: in 1990, almost all surface waters in the European Arctic had critical levels of acidity due to sulfur emissions from lower latitudes (AMAP 2006). Additionally, the chemical composition of Arctic snowpack is directly tied to Arctic haze periods with increased pollution loading (Sharp 2002, Douglas and Sturm 2004). Thus, wintertime decreased concentrations of sulfate and nitrate aerosol at Utqiaġvik may decrease acidifying pollutant uptake into ecosystems on the surface.

While the Arctic haze phenomenon is mostly driven by long-range transport of air pollution from lower latitudes, naturally produced sea salt aerosol species also play an important role in aerosol particle mass and scattering properties (Quinn et al. 2002). Figure 10 shows the time series for chloride (Cl^-) and sodium (Na^+)

concentrations, showing that submicron sea salt aerosol species peak in the haze season. This is likely due to long-range transport of fine sea salt particles from lower latitudes and local lofting of submicron particles from snowpack and frost flowers (Quinn et al. 2002, Jacobi et al. 2009, Jacobi et al. 2012). Conversely, supermicron chloride and sodium concentrations peak in the summer and dominate aerosol particle mass (figure 10), which is consistent with the local primary production of coarse sea salt aerosol (Quinn et al. 2002, May et al. 2016).

Further analysis of sea salt aerosol composition was done in two ways: 1) via direct measurements of sodium and chloride aerosol species (figure 11) and 2) via linear regressions of Cl^-:Na^+ molar ratios to probe for pH-dependent chloride depletion (figures 11, 12, and 13). Chloride depletion is quantified by comparing measured chloride: sodium ion ratios to the expected ratio in Arctic seawater, which is approximately 1.16 at Utqiaġvik (Feng et al. 2017, May et al. 2016). Lower Cl^-:Na^+ ratios than this value show that acid-driven chloride depletion is occurring. Thus, the measured Cl^-:Na^+ molar ratio can be an effective indicator of pH-dependent aerosol transformation mechanisms (Feng et al. 2017, Hara et al. 2002).

From the MAKESENS model, haze season submicron sodium and chloride concentrations appear to be increasing by 1.1% and 0.96% respectively (figure 11). Since submicron sea salt aerosol is a major contributor to aerosol particle mass and submicron scattering in the haze season, increases over time could affect aerosol chemical composition and optical properties (Feng et al. 2017, Quinn et al. 2002, Struthers et al. 2011). The haze season linear regressions in figure 12 compare the measured Cl^-:Na^+ ratio from this study with the seawater ratio. The submicron

regression shows that the measured Cl^-:Na^+ ratio agrees with the seawater ratio, even though submicron non-sea salt sulfate and nitrate peak in the same time frame (figure 12). Since chloride depletion is acid-dependent, higher concentrations of nss $SO_4^=$ and NO_3^- would be expected to increase chloride depletion in the haze season, however, the regressions in figure 12 do not support this theory. Increased haze season transport from the Pacific sector, as discussed in section 3.2, could explain the increase in submicron sea salt species concentrations and Cl^-:Na^+ ratios that match those found in seawater (figures 11 and 12). It is hypothesized that chloride depletion is still occurring to a minor extent in the haze season, but the effect is offset by enhanced long-range transport of sea salt aerosol particles.

Simultaneously, haze season supermicron sodium and chloride concentrations seem to be decreasing by -4.1% and -5.6% respectively but are not statistically significant (figure 11). The supermicron Cl^-:Na^+ regression does not indicate that chloride depletion is occurring in the haze season since the regression also falls on top of the expected seawater ratio (figure 12); therefore, neither of the haze season regressions in figure 12 indicate that haze season chloride depletion is occurring

In the summer, sodium and chloride concentrations suggest a similar pattern as the haze season concentrations; again, data suggests that submicron sodium and chloride concentrations are increasing (0.78% and 0.80% respectively) with supermicron concentrations decreasing (-0.67% and -0.52% respectively), though, again, these trends are not statistically significant. Both submicron and supermicron Cl^-:Na^+ ratios in the summer regressions show more separation from the seawater

ratio than the haze season regressions (figure 13), however, these trends may not be representative of atmospheric conditions due to several seemingly influential chloride measurements observed on the regression.

Outlier tests to inspect the samples for low volumes or anomalous measurements for other chemical species did not indicate that these samples should be omitted from the data set, but clear divergence from the range of normal chloride concentrations could still be due to measurement error. Summer season measurements in this study are less robust towards influential values than the haze season since there are significantly fewer samples (see section 2.1). Both regressions have several measurements where chloride concentrations are so low that they may be influencing the overall trend line (figure 13). Due to uncertainty with the time-scale in this study and variability of summer aerosol measurements, more years of measurements are needed to verify trends in summertime sea salt aerosol concentrations and Cl^-:Na^+ ratios. Measurements at Utqiaġvik extend to current times, so analysis of aerosol measurements between 2013-2021 may confirm or counter this observation.

Observed summertime sea salt aerosol trends counter expected consequences of a warming Arctic (Struthers et al. 2011); this trend is especially confounding since supermicron biogenic non-sea salt sulfate appears to be increasing in this study (figures 3 and 10). Since primary production of sea salt aerosol happens on the ocean's surface, increased concentrations in supermicron sea salt aerosol and non-sea salt sulfate should be associated. Increased SSTs, reduced sea ice cover, and prolonged melt seasons are both known to enhance DMS

fluxes from the ocean and are favorable for sea salt aerosol production (Quinn et al. 2002, Quinn et al. 2008, Sharma et al. 2012, May et al. 2016). The decrease in supermicron sea salt aerosol species was an unexpected result in this study and merits more attention to validate if this trend is significant. Further analysis of chemical measurements between 2013 to 2020 may provide more insight regarding this uncertain result.

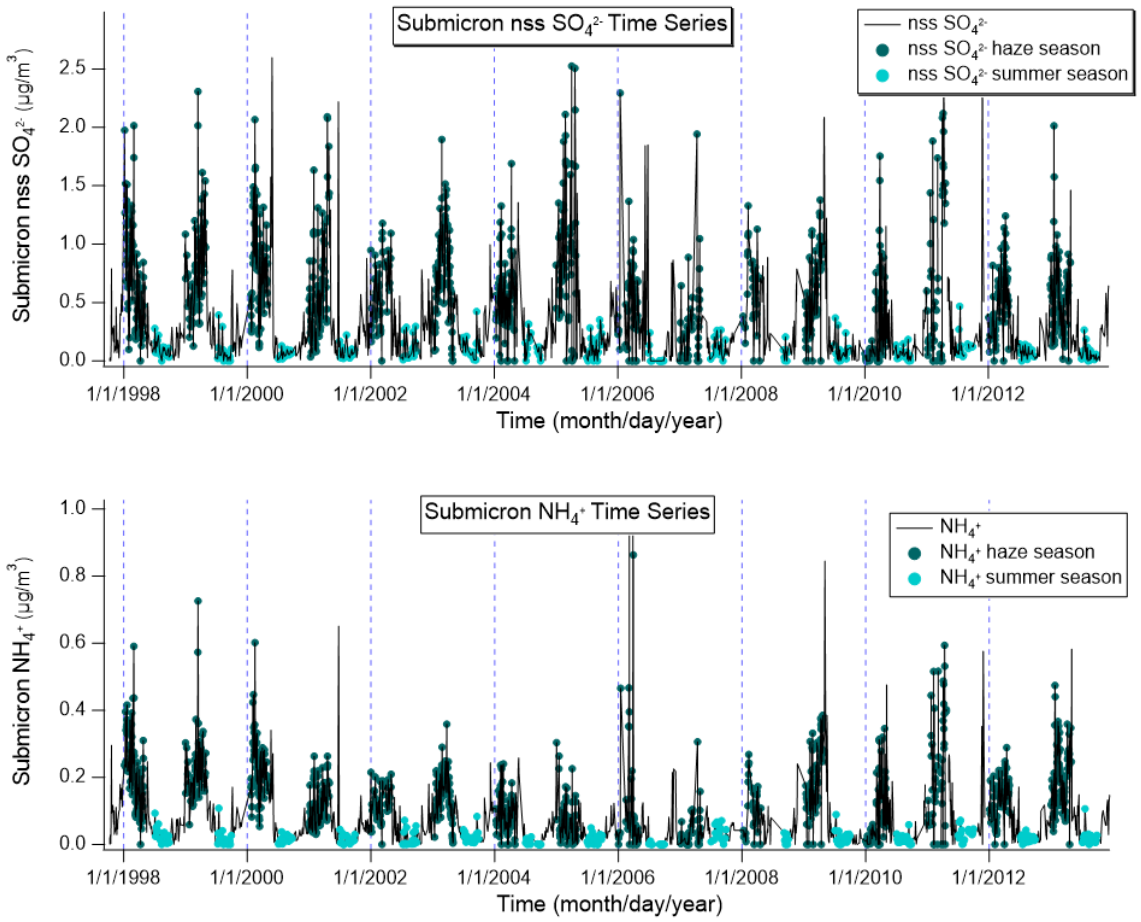

Figure 2: Time series for (a) non-sea salt sulfate (µg/m^3) and (b) ammonium (µg/m^3) concentrations at Barrow Observatory exhibit seasonal maximums of species concentrations in the haze season. The dark teal circles represent data from the haze season (January-April) and the light blue circles represent data from the summer season (July-September). Concentrations are presented in µg/m^3 on the y-axis.

Submicron Non-sea Salt Sulfate Haze Season

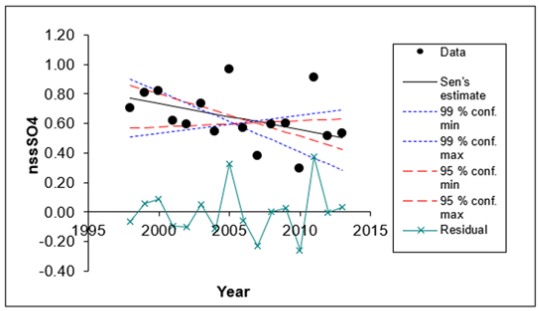

Submicron Non-sea Salt Sulfate Summer Season

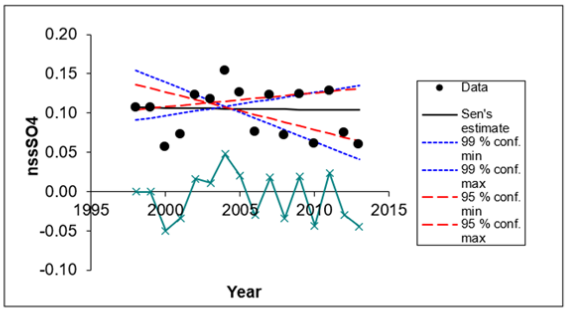

Supermicron Non-sea Salt Sulfate Haze Season

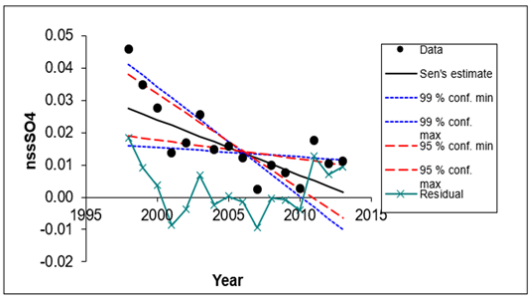

Supermicron Non-sea Salt Sulfate Summer Season

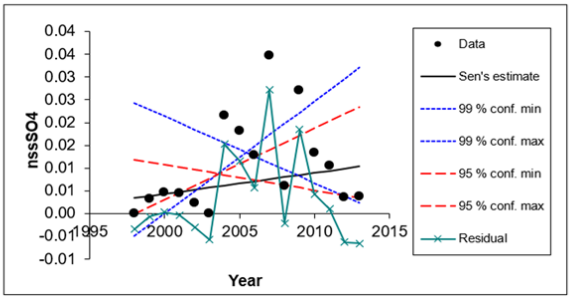

Seasonal Trends in Seasonal Non-sea Salt Sulfate (1998-2013)				
Season	**Particle Size**	**Significance**	**Sen's Slope**	**% change**
Haze	Submicron	90%	-2.00 E-02	-2.9%
Haze	Supermicron	99%	-1.62E-03	-12%
Summer	Submicron	-	-5.98 E-04	0.0%
Summer	Supermicron	-	4.61 E -04	9.7%

Figure 3: The MAKESENS model for non-sea salt sulfate concentrations from 1998-2013 indicates that haze season concentrations of sulfate are decreasing for submicron and supermicron particles. P-values are less than 0.1 and 0.01 respectively. Sen's slope estimates for non-sea salt sulfate concentrations indicate a decreasing trend for summer submicron particles and an increasing trend for summer supermicron particles, but neither of these trends is statistically significant.

Submicron Ammonium Haze Season

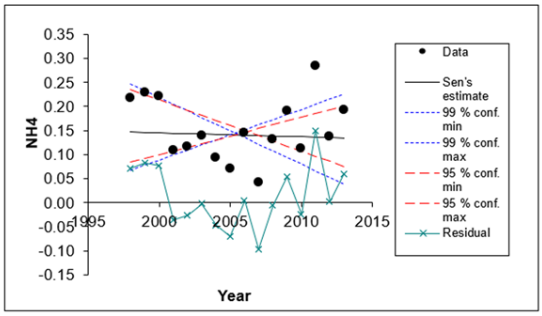

Submicron Ammonium Summer Season

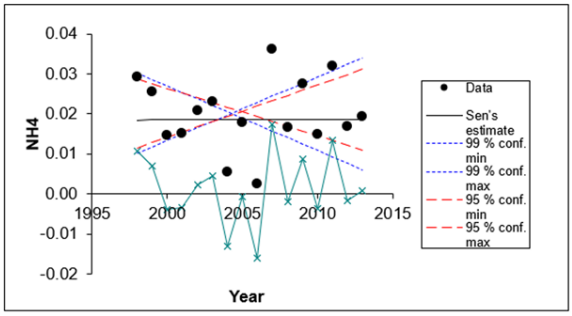

Seasonal Trends in Submicron Ammonium (1998-2013)				
Season	**Particle Size**	**Significance**	**Slope**	**% change**
Haze	Submicron	-	-1.70 E -03	-0.60%
Summer	Submicron	-	1.25 E-04	0.0%

Figure 4: The MAKESENS model did not detect any significant trends in submicron ammonium concentration for either season from 1998 to 2013. Ammonium is only reported for submicron particles because concentrations of ammonium are below the detection limit for supermicron particles.

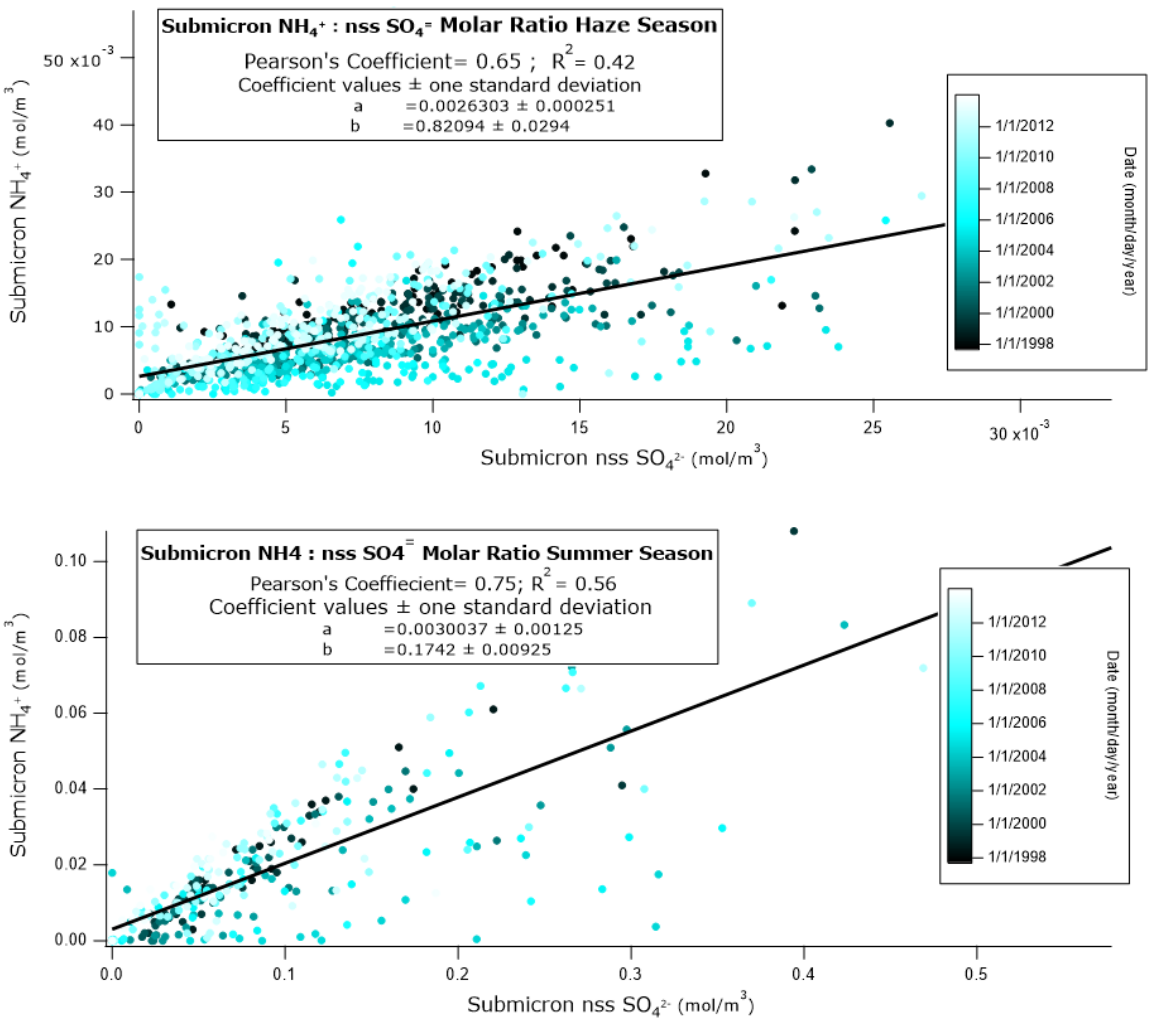

Figure 5: Linear regressions of submicron ammonium vs non-sea salt sulfate in the haze and summer seasons from 1998 to 2013 showed a moderate correlation between the two species. The R^2 values for the molar ratios are 0.42 in haze season and 0.56 in the summer. P-values are less than 0.001 for both regressions.

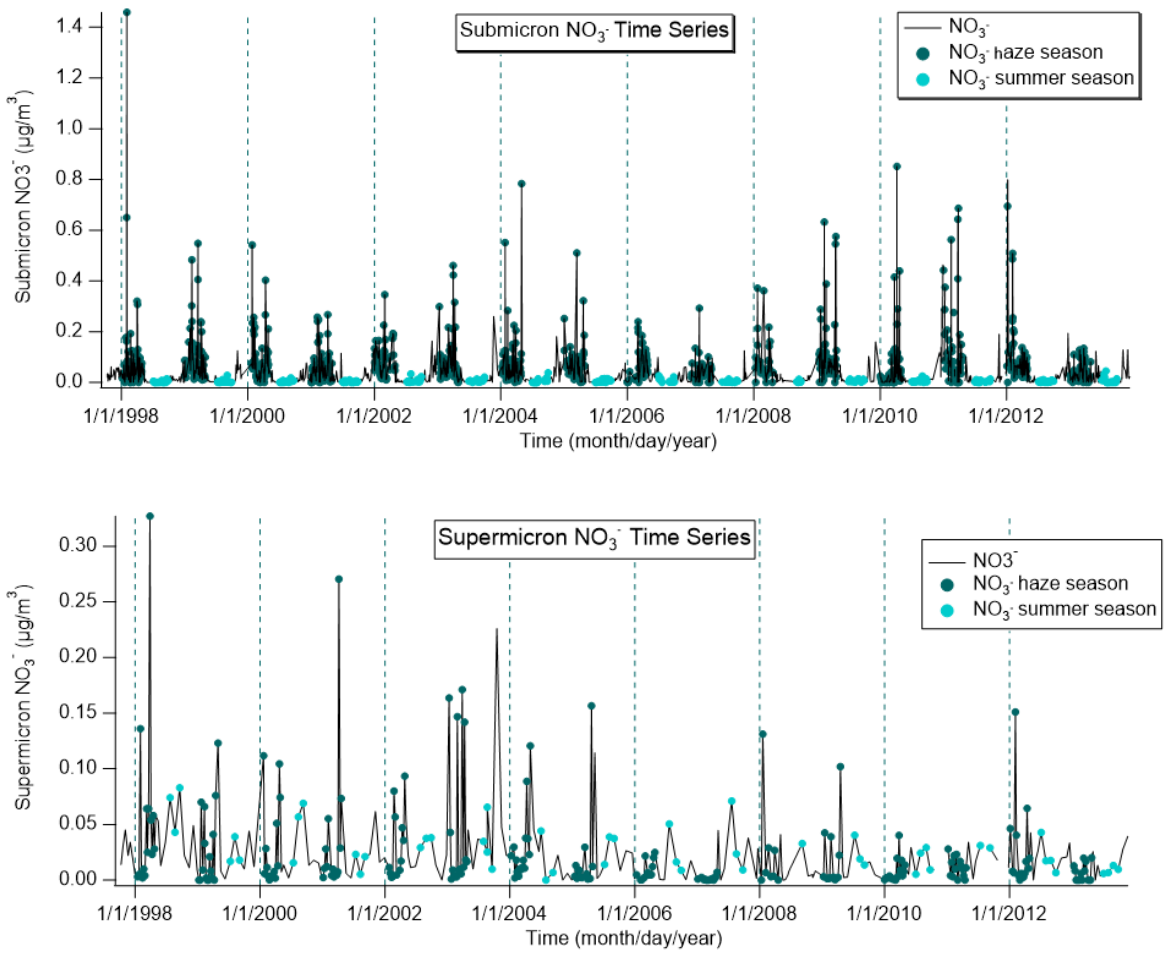

Figure 6: Time series for (a) submicron nitrate concentrations and (b) supermicron nitrate concentrations. The dark teal circles represent haze season nitrate concentrations and the light blue circles represent summer season nitrate concentrations. Concentrations are presented in µg/m^3 on the y-axis.

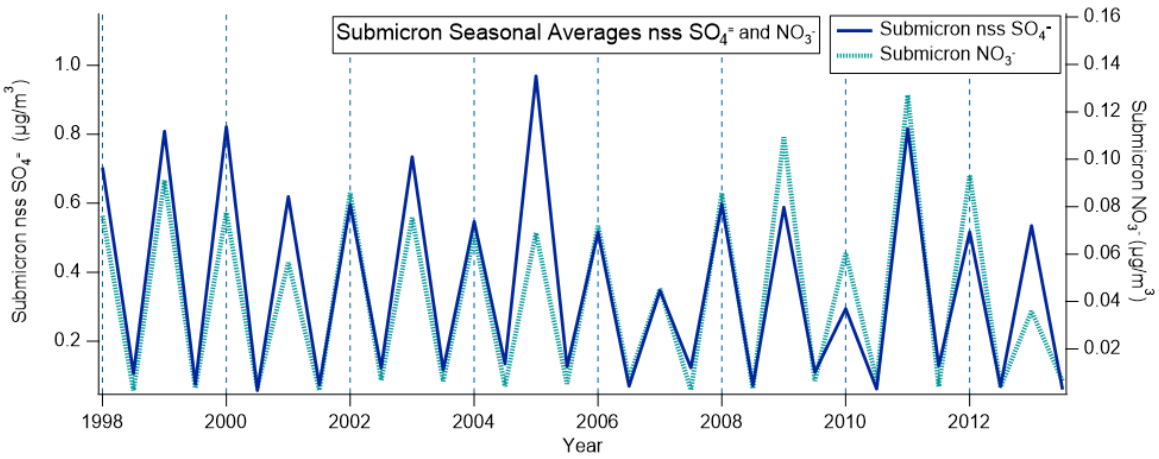

Figure 7: The time series for seasonal averages of submicron non-sea salt sulfate and nitrate exhibits a sawtooth pattern for both species. Spikes in concentration correspond with the haze season and dips correspond with the summer. The left y-axis shows submicron nss sulfate concentrations and the right y-axis shows submicron nitrate concentrations. Seasonal averages of nss $SO_4^=$ are indicated by the solid blue line and NO_3^- seasonal averages correspond to the light blue dashed line.

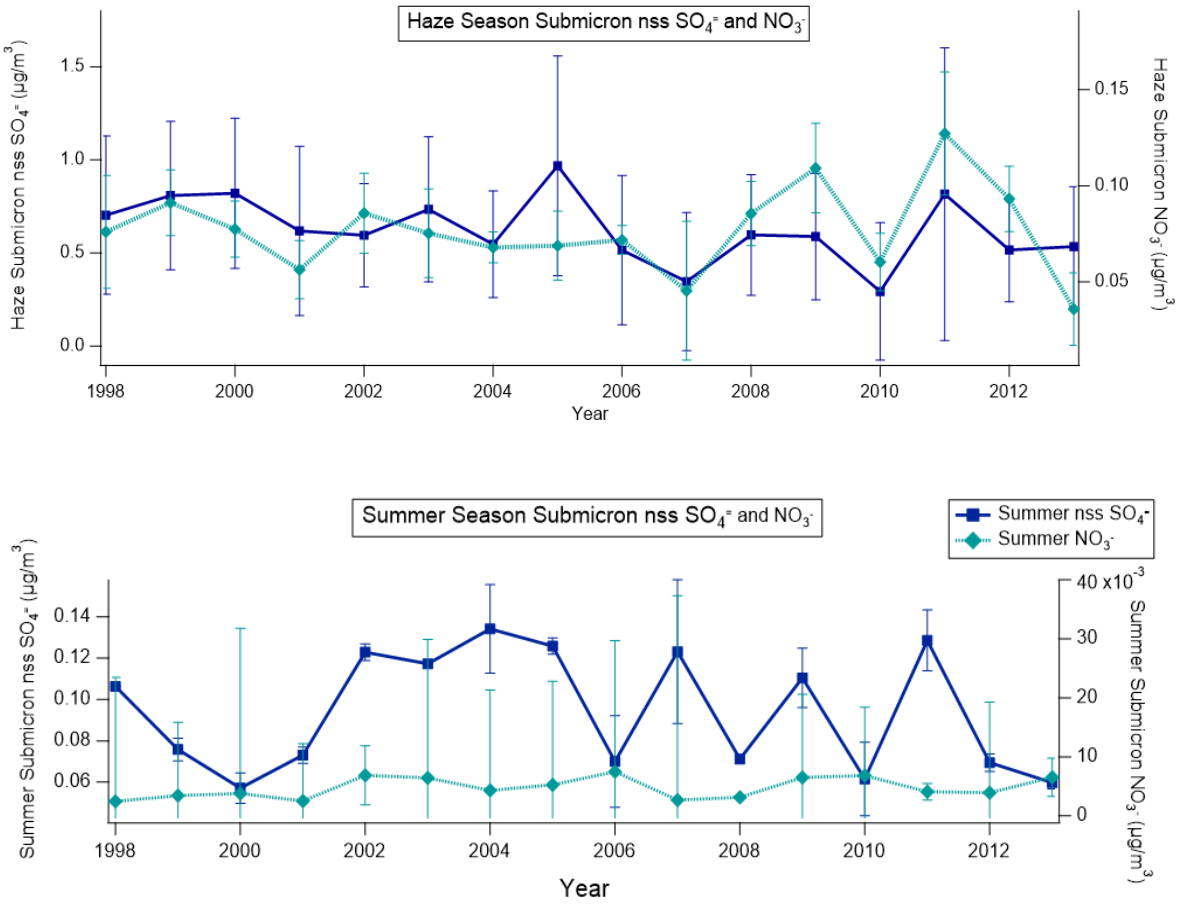

Figure 8: (a) Haze season and (b) summer season averages for submicron non-sea salt sulfate (dark blue solid line) and nitrate (light blue dashed line). The error bars show the standard deviation for the calculated seasonal averages which indicates the variability of chemical measurements within a season. Nss sulfate concentrations are on the left y-axis and nitrate concentrations are on the right y-axis.

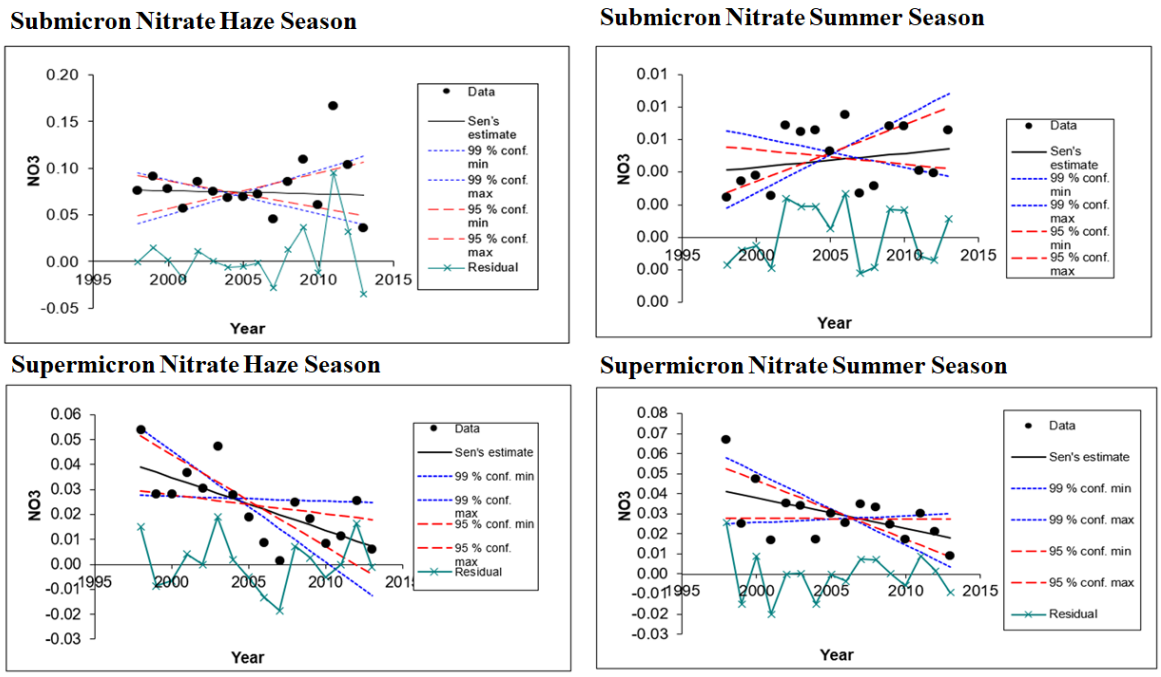

Seasonal Trends in Nitrate (1998-2013)				
Season	Particle Size	Significance	Sen's Slope	% change
Haze	Submicron	-	-3.47 E-04	0.0%
Haze	Supermicron	99%	-2.12 E -03	-8.2%
Summer	Submicron	-	8.53 E -05	0.0%
Summer	Supermicron	95%	-1.54 E -03	-6.89%

Figure 9: Seasonal trends for supermicron nitrate are among the most significant changes in chemical composition at Utqiaġvik. The decreases for supermicron nitrate are 99% significant in the haze season and 95% significant in the summer.

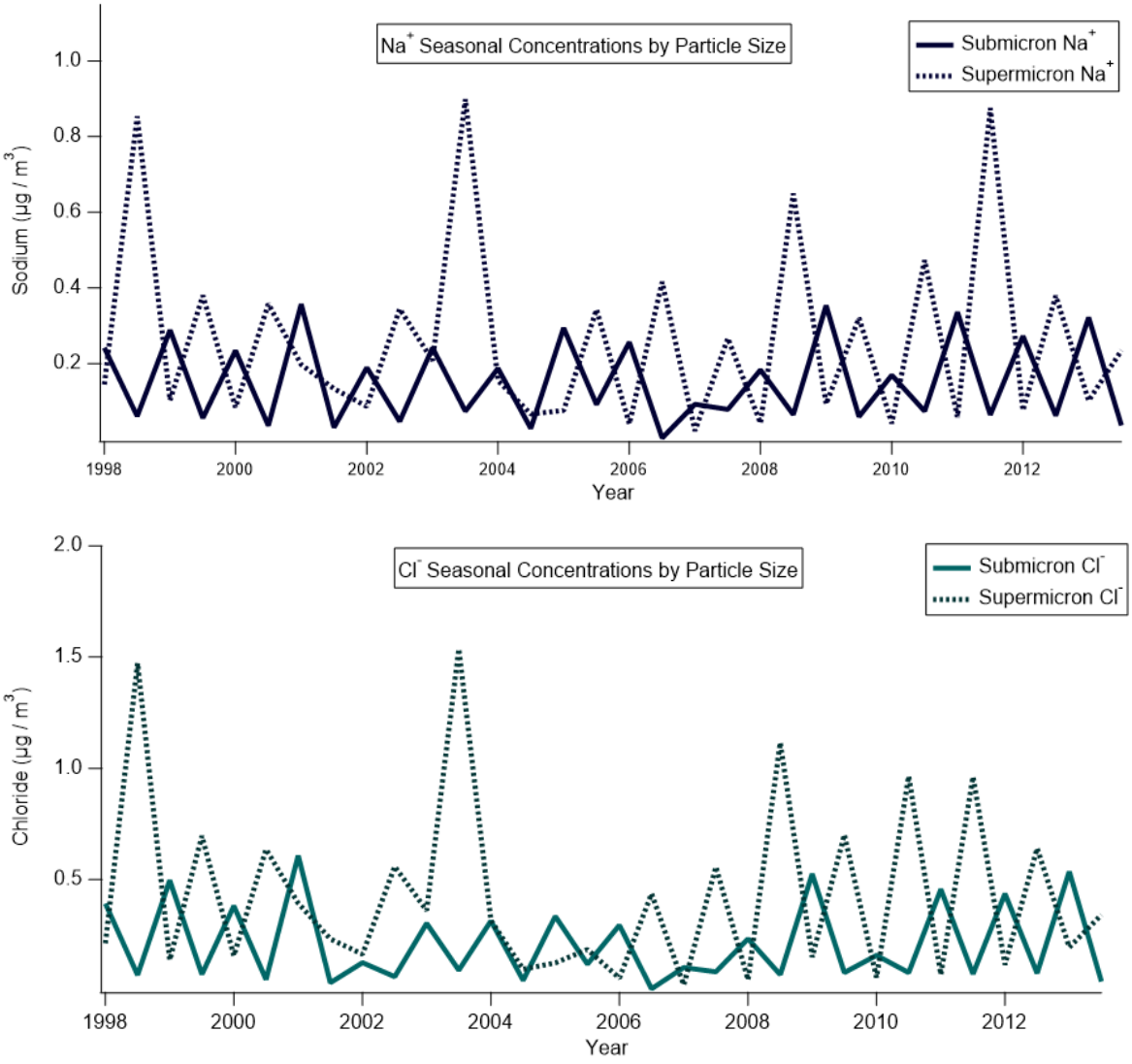

Figure 10: Time series of seasonal averages of (a) sodium ion and (b) chloride ion concentrations from 1998 to 2013. The solid lines correspond to submicron concentrations of the two species and the dashed lines correspond to supermicron concentrations. Submicron sea salt ion concentrations peak in the haze season and dip in the summer. Supermicron sea salt ion concentrations peak in the summer.

Seasonal Trends in Sodium (1998-2013)				
Season	Particle Size	Significance	Sen's Slope	% change
Haze	Submicron	-	2.72E-03	1.1%
Haze	Supermicron	-	-3.88E-03	-4.1%
Summer	Submicron	-	4.25E-4	0.78%
Summer	Supermicron	-	-2.95E-03	-0.67%

Seasonal Trends in Chloride (1998-2013)				
Season	Particle Size	Significance	Sen's Slope	% change
Haze	Submicron	-	3.44E-03	0.96%
Haze	Supermicron	-	-9.12E-03	-5.6%
Summer	Submicron	-	5.42E-04	0.80%
Summer	Supermicron	-	-3.66E-03	-0.53%

Figure 11: The MAKESENS model did not detect any significant trends in sodium and chloride concentrations for any particle size or season from 1998 to 2013. In general, there seem to be small increases in submicron sea salt species and decreases in supermicron sea salt seasons in both seasons, but more data is needed to demonstrate that these tentative trends are statistically significant.

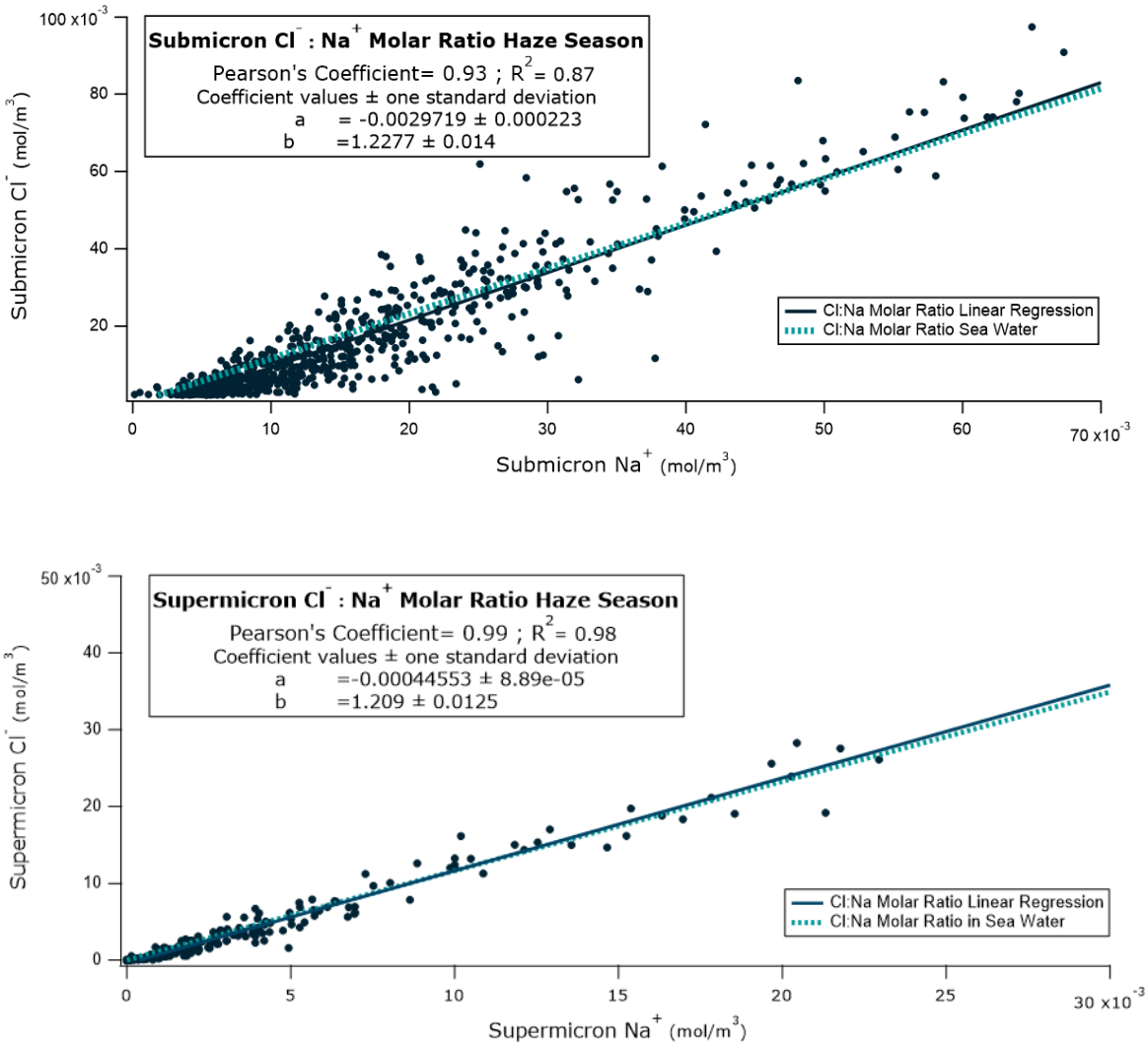

Figure 12: Haze season Cl^-:Na^+ ion molar ratios show a strong correlation for both particle sizes. The R^2 for submicron and supermicron particles are 0.87 and 0.98 respectively. P-values are < 0.001 for both regressions. The expected chloride to sodium ratio of 1.16 in seawater was used to approximate trends in chloride depletion, which is tied to aerosol acidity. The blue dashed line shows the Cl^-:Na^+ ratio present in seawater (1.16) and the solid dark blue regression lines depict the measured atmospheric ratio for both particle sizes at Utqiaġvik, AK.

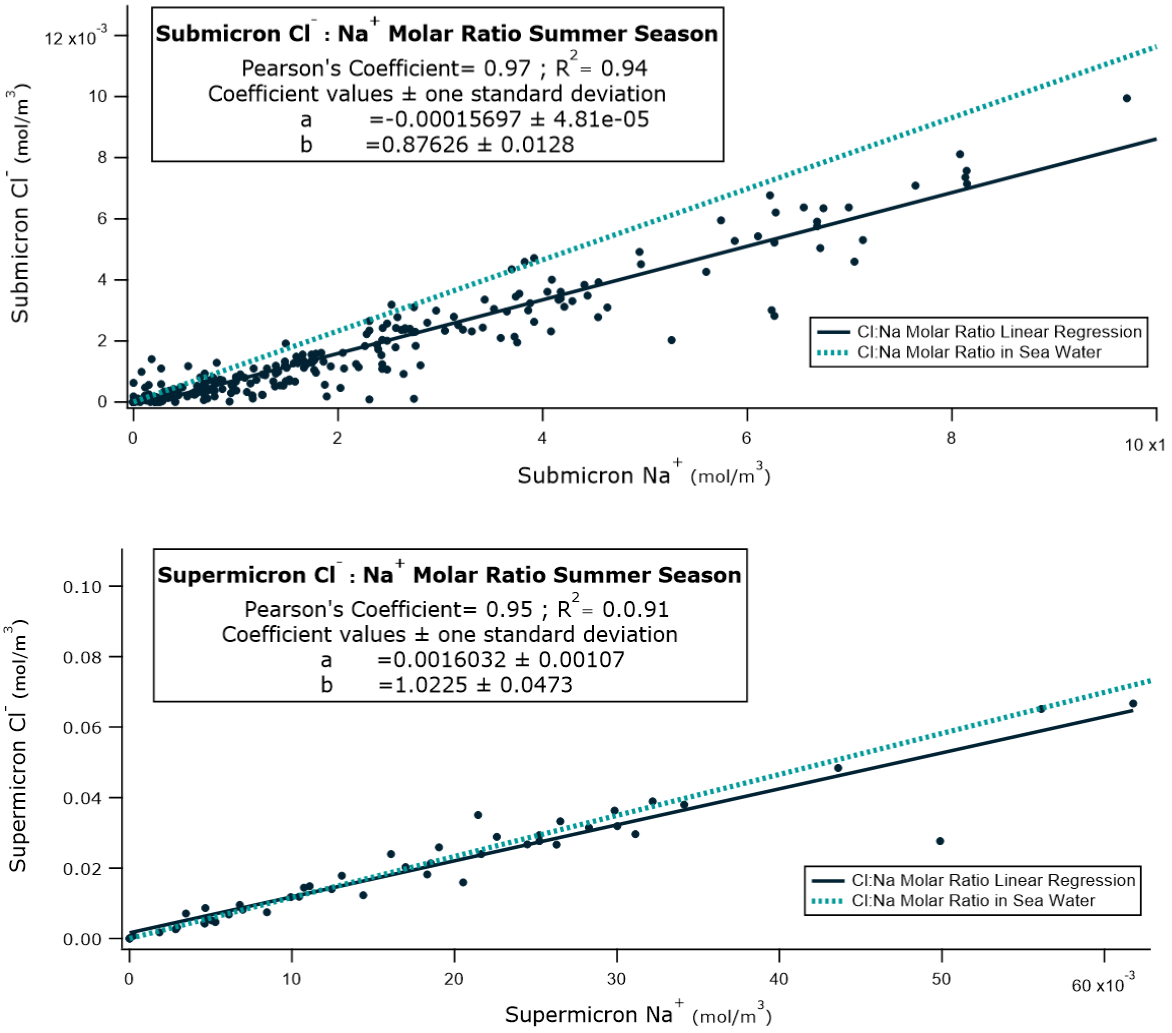

Figure 13: Summer season Cl^-:Na^+ ratios for submicron and supermicron particles. The light blue dashed line is the expected ratio of Cl^-:Na^+ of 1.16 in seawater and the dark blue trend lines are the measured ratio at Utqiaġvik for both particle sizes. R^2 values are 0.94 for submicron particles and 0.91 for supermircon particles. P-values are < 0.001 for both regressions.

3.2 Trends in emissions and atmospheric transport to Utqiaġvik

Atmospheric transport modeling and emission reductions contextualize trends in chemical composition at Utqiaġvik over the last several decades. The five sectors in this study were separated by longitude coordinates from the origin at the North Pole, see section 2.3 (figure 1). The primary regions for transport to Utquiagvik between 1998 and 2020 are the North American and Russian/Asian sectors (figure 14), which together account for 63% of transport to Utquiagvik. The Atlantic, Europe, and Pacific sectors contribute to the remaining proportion of atmospheric transport (figure 14). The bar chart in figure 15 also shows North America and Russia / Asia as dominant transport sectors for both seasons.

Though the European sector contributes 14% of total transport to Utqiaġvik overall, long-term trends in transport and emissions reductions are likely causing the decreased nss $SO_4^=$ concentrations discussed in section 3.1 (figures 14 and 15). Figure 16 shows a 95% significant decrease in transport from the European sector during the haze season for arrival heights of 10m (-2.0% decrease) and 100m (-1.7% decrease). Besides the decrease in transport, emissions from Europe have decreased significantly. Sulfur dioxide emissions peaked in the late 1900s in North America and Europe, but have since decreased with regulations imposed to assuage mounting concerns about acid rain and health effects of industrial air pollution (Klimont et al. 2012, Tørseth et al. 2012, Hidy et al. 2016, Quinn et al. 2007). Several studies estimate that SO_2 emissions in Europe have decreased by approximately 6100 gigatons (-41%) since 2000 (Klimont et al. 2012, Tørseth et al. 2012). Due to these species' short lifetimes of around one week, sulfur oxides, which are

precursors for non-sea salt sulfate, respond quickly to changes in emissions (Hidy et al. 2016, Yang et al. 2018).

No changes in haze season transport from North America were detected in this study; however, it's possible emissions reductions from North America are also contributing to the observed decrease in nss $SO_4^=$. SO_2 emissions from North America decreased by 1447 gigatons from 2000 to 2005 and 6660 gigatons from 2005 to 2010 (Klimont et al. 2012). SO_2 emissions contributions from these two sectors have been eclipsed in the 21st century by emissions from Eastern Europe, Central Asia, and international shipping (Klimont et al. 2012, Tørseth 2012, Yang et al. 2018). The rate of increased SO_2 emissions from Eastern Europe and Asia is slower than emission decreases from Western and Central Europe and North America, so the result is a net decrease in SO_2 emissions (Klimont et al. 2012, Hidy et al. 2016). Historical decreases in SO_2 emissions in Europe and North America coupled with the statistically significant haze season decrease in transport from Europe likely explain the decrease in measured nss $SO_4^=$ at Utqiaġvik.

Simultaneously, the Pacific sector has shown an unexplained increase in transport in the haze season at 10m (4.3% increase, 99.9% significance) and 100m (3.7% increase, 99% significance) which is among the strongest changes in transport to Utqiaġvik (figure 17). Transport from the Pacific in the haze season is strongest for the 1000m arrival height making up 19% of sector transport to that altitude (figure 14), however, transport at the two lower arrival heights, which make up 10-11% of transport is increasing (figure 17). Since the Pacific sector exhibits a large surface area of open ocean, it is reasonable to conclude that the increases in

submicron sodium and chloride aerosol could be due to the significant increase in transport from the Pacific sector (figure 17).

The cause for the increase in Pacific transport in the haze season is unclear, as ties to atmospheric and oceanic oscillation patterns are not obvious. Pacific Decadal Oscillation is an important, persistent oceanic oscillation pattern that often explains oceanic and atmospheric climatological processes and decadal variability in the Central and North Pacific (Mantua and Hare 2002, Schneider and Cornuelle, 2005). Trends in transport from the Pacific sector were compared with seasonal averages of Pacific Decadal Oscillation (PDO) patterns by plotting time series and performing linear regressions. PDO periods are defined according to sea surface temperature (SST) anomalies (Matua 1999). PDO temperature anomalies were accessed from 1997 through winter of 2020 and averaged between January-April for haze season to correspond with Pacific sector transport trends (NOAA NCEI PDO index 2020). The time series of the seasonal averages did not show proportional relationships between these two variables since temperature anomalies did not correspond with seasonal trends in transport at 10 and 100m (figure 18). Furthermore, the regressions between Pacific transport did not show a significant correlation, with R^2 values of 0.11 and 0.088 respectively (figure 18). These results suggest it is unlikely the increase in transport from the Pacific sector is tied to Pacific Decadal Oscillation.

Alternatively, the enhanced transport from the Pacific sector could be a consequence of the weakening of the Arctic front, which has been observed in several studies over the past few decades (Stohl 2006, AMAP 2008, Quinn et al.

2008, Fisher et al. 2011). As the Arctic warms, a decrease in the temperature gradient between the Arctic and lower latitudes has weakened the Arctic front (AMAP 2008). This phenomenon can escalate and create long-range transport pathways for aerosol pollution to the Arctic (Quinn et al. 2008, AMAP 2008). Increased haze season transport from the Pacific sector may suggest increased concentrations of sea salt aerosol at Utqiaġvik; however, uncertainty about these processes remains.

Summer HYSPLIT trends from the North America and Russia / Asia sectors also provide insight into how atmospheric transport is changing for those sectors (figures 19 and 20). Strong decreasing trends occurred for North American transport in the summer at 10m arrival height (-2.6% decrease, 99.9% significance) and 100m arrival height (-1.9% decrease, 95% significance (figure 19). Simultaneously, transport from the Russian and Asian sector showed significant increases at 10m (1.8% increase, 95% significance), 100m (1.6% increase, 95% significance), and 1000m (1.1% increase, 90% significance) (figure 20).

Due to the episodic nature of summertime burning events, specific case studies are needed to provide direct ties between terrestrial and atmospheric processes; however, since wildfires are expected to be exacerbated by climate change, long-term trend analysis can reveal how increased frequency and intensity of fire events may be affecting aerosol composition and optical properties at Utqiaġvik (IPCC 2013, Ren et al. 2020, Shen 2017, Stohl 2006, Stohl 2007). Summertime processes of interest for biomass burning include long-range transport of fire plumes from lower latitudes. Fires in Siberia are a significant source of

summer black carbon in the Arctic and agricultural fires in Eastern Europe and Northern Asia have been proven to increase aerosol optical depth and influxes of black carbon (Stohl 2006 and 2007). Case studies that connect fire events with changes in aerosol properties can be done by tying spikes in chemical tracer species and aerosol absorption to individual back trajectories. For example, non-sea salt potassium, a chemical tracer species for fire events, is among the cations measured at Utqiaġvik. Spikes in nss potassium can be coupled with individual back trajectories and documented fires to determine direct pollutant sources. An influx of black carbon and soot from natural and prescribed burns also spike aerosol light absorption in the Arctic, so optical measurements can be used to identify summertime burning events. Long-term transport modeling in this study only offers limited insight into summertime aerosol processes so nss potassium measurements and in-depth analysis of trends of absorption at Utqiaġvik are needed to assess the direct effect summertime burning events may have on aerosol composition at Utqiaġvik.

Average Time Fraction in Five Sectors by Arrival Height 1997-2020					
Arrival Height	Pacific	Russia / Asia	Europe	Atlantic	North America
10 m	10%	33%	14%	19%	24%
100 m	11%	35%	14%	17%	35%
1000 m	19%	33%	10%	9%	30%

Figure 14: Table showing sector distributions for the three arrival heights (10m, 100m, and 1000m). Russia / Asia and North America are the primary sectors making up roughly 60% of transport to Utquiagvik followed by the Atlantic, the Pacific, and Europe.

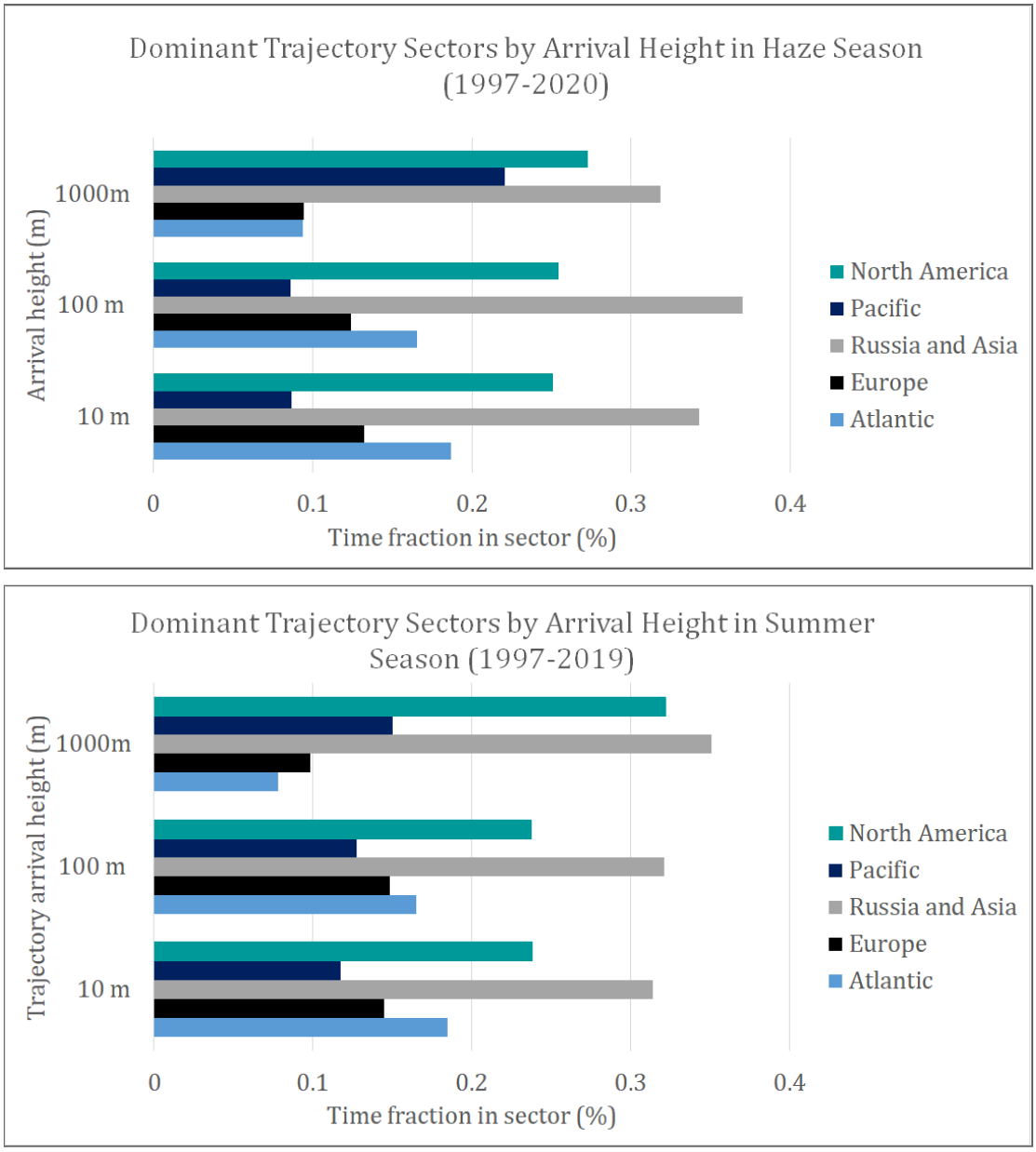

Figure 15: Bar charts denoting seasonal averages for atmospheric transport to Utquiagvik with (a) showing haze season distributions and (b) showing summer season. From top to bottom, North America (teal), the Pacific (dark blue), Russia and Asia (gray), Europe (black), and the Atlantic (light blue) are pictured. Charts are separated by arrival height on the y-axis and time fractions for each sector on the x-axis. Long-term trend analysis from 1997 to 2019 shows that haze season transport for the Europe sector has decreased at 10 and 100m arrival heights while Pacific transport has increased at 10 and 100m. Summer season transport from North America decreased at 10 and 100m while Russia/Asia transport is increasing for all three arrival heights.

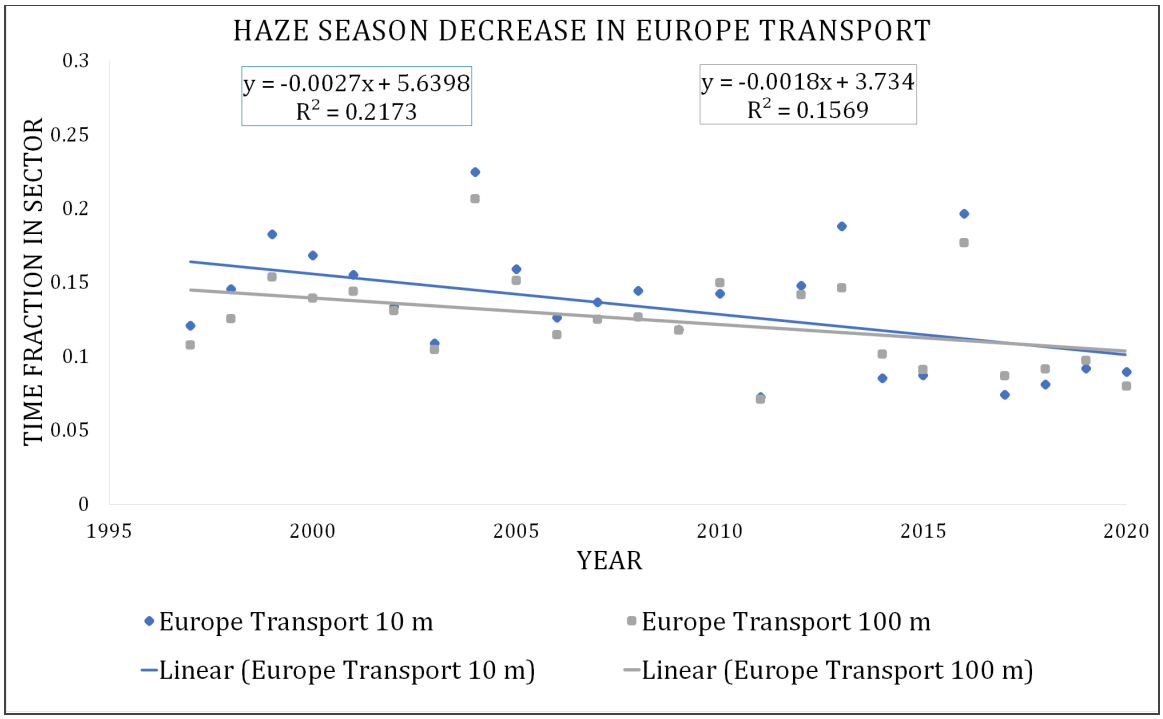

Sector, Season, and Arrival Height	Significance	Sen's Slope	R^2	% change
Europe Haze at 10m	95%	-0.003	0.22	-2.0%
Europe Haze at 100m	95%	-0.003	0.16	-1.7%

Figure 16: There has been a 95% significant decrease in haze season transport for the Europe sector. The regression above shows negative slopes for both arrival heights with weak correlation in R^2 values with 0.22 for 10m and 0.16 for 100m. This result combined with emission reductions in Europe and North America likely caused the decreases in haze season non-sea salt sulfate and nitrate concentrations at Utqiaġvik.

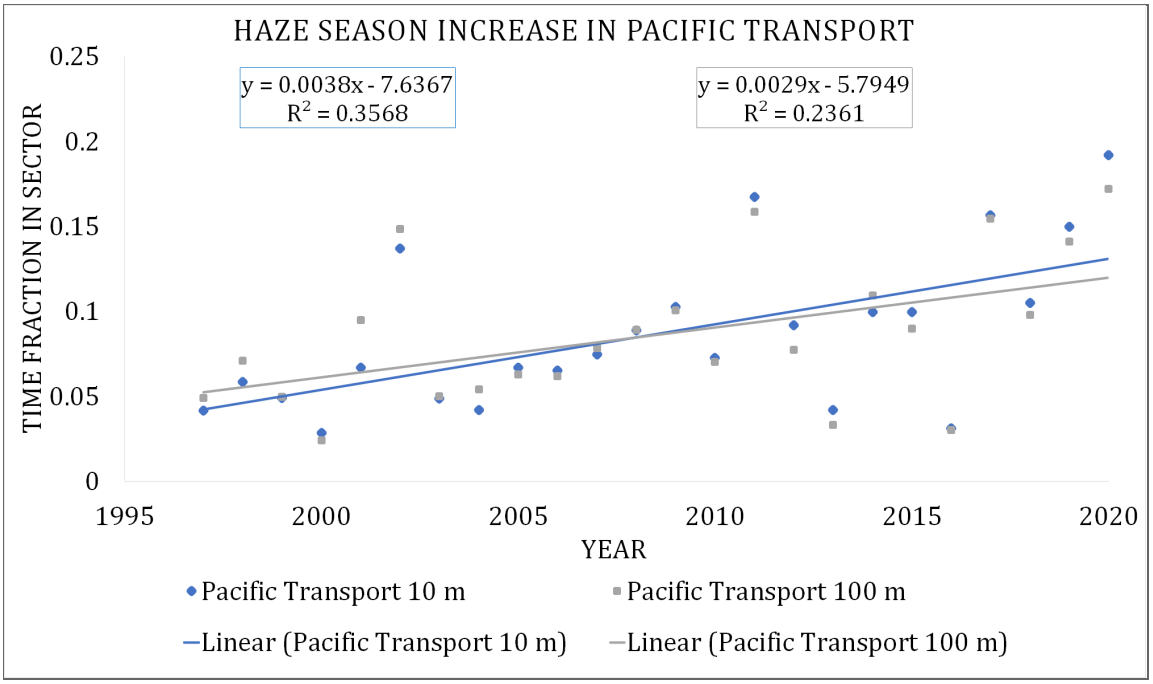

Sector, Season, and Arrival Height	Significance	Sen's Slope	R^2	% change
Pacific Haze at 10m	99.9%	0.004	0.36	4.3%
Pacific Haze at 100m	99%	0.003	0.24	3.7%

Figure 17: Pacific transport in haze season has increased with 99.9% significance for 10m arrival height and 99% significance for 100m arrival height. Sen's slope estimates suggest a positive association for Pacific transport over time. R^2 values of 0.36 for 10m arrival height and 0.24 for 100m show a relatively stronger correlation for Pacific sector trends than for Europe sector trends. The increase in transport from the Pacific sector may be tied to sea salt aerosol enrichment in the haze season and a stronger correlation between Cl^-:Na^+ sodium ion molar ratios than expected (figures 11 and 12).

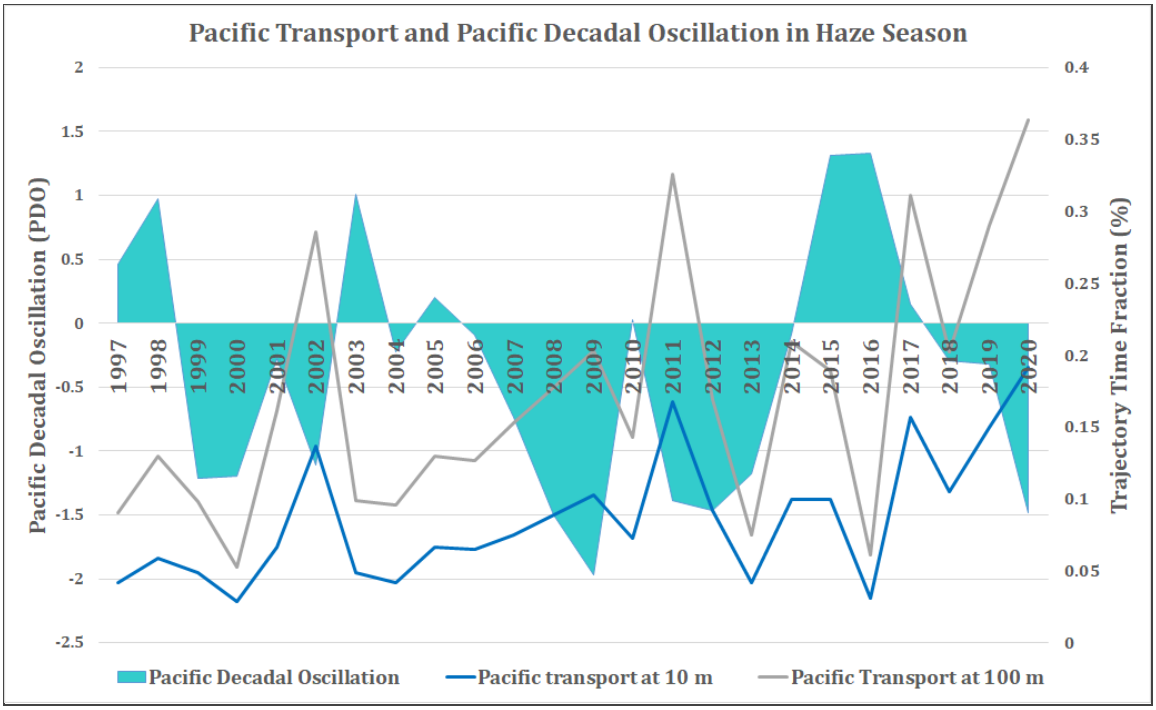

Pacific Transport vs. Pacific Decadal Oscillation			
Regression	**R^2**	**Significance**	**Conclusion**
Pacific Transport at 10m vs. PDO	0.11	-	No association
Pacific Transport at 10m vs. PDO	0.089	-	Not association

Figure 18: Trends in haze season Pacific sector transport were compared to Pacific Decadal Oscillation (PDO) patterns to determine if the two processes are connected. A time series for PDO temperature anomalies (teal shading) and time fractions for Pacific sector transport (blue line= 10m and gray line=100m) is presented above. PDO and Pacific sector transport does not seem to be related processes since annual increases in the Pacific do not seem to correspond to annual temperature anomalies. This conclusion is confirmed by the two regressions shown in the table below, where R^2 values were 0.11 for 10m arrival height and 0.089 for 100m arrival height. Thus, increased haze season transport from the Pacific sector is not explained by Pacific Decadal Oscillation patterns.

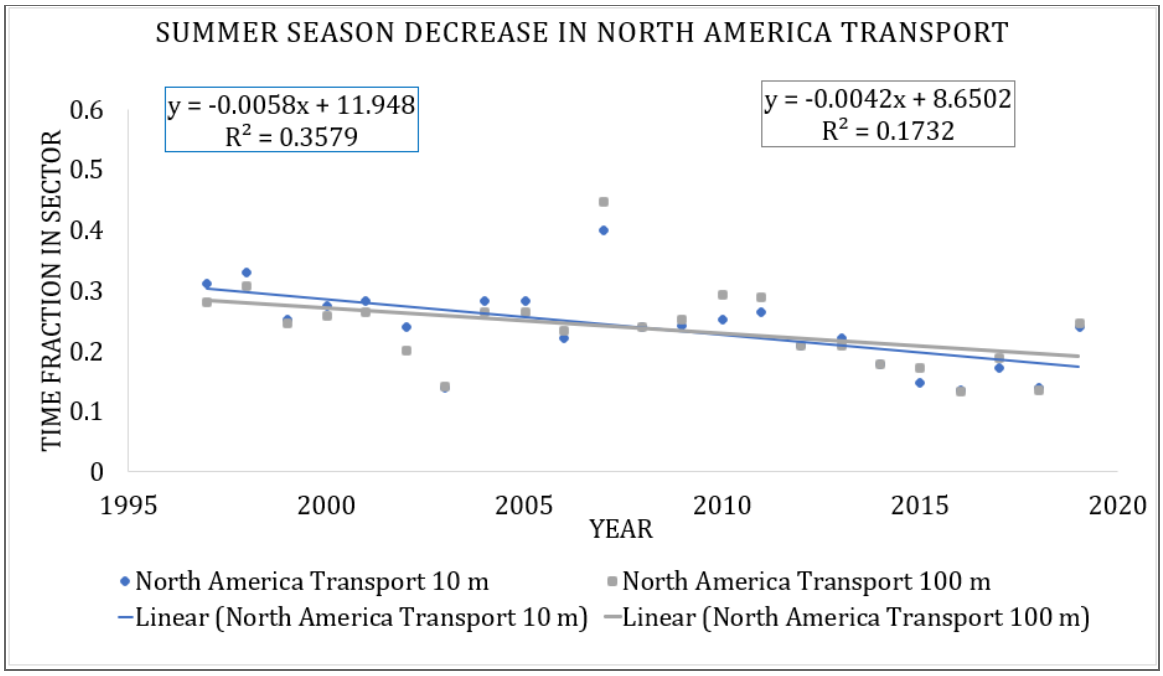

Sector, Season, and Arrival Height	Significance	Sen's Slope	R^2	% change
N America Summer at 10m	99.9%	-0.006	0.36	-2.6%
N America Summer at 100m	95%	-0.003	0.17	-1.9%

Figure 19: Summer trajectory analysis shows a decrease in N America transport with 99.9% significance for 10m and 95% significance for 100m. Sen's slope estimates show a negative association for 10 m and 100m arrival heights and R^2 values are 0.36 and 0.17 respectively.

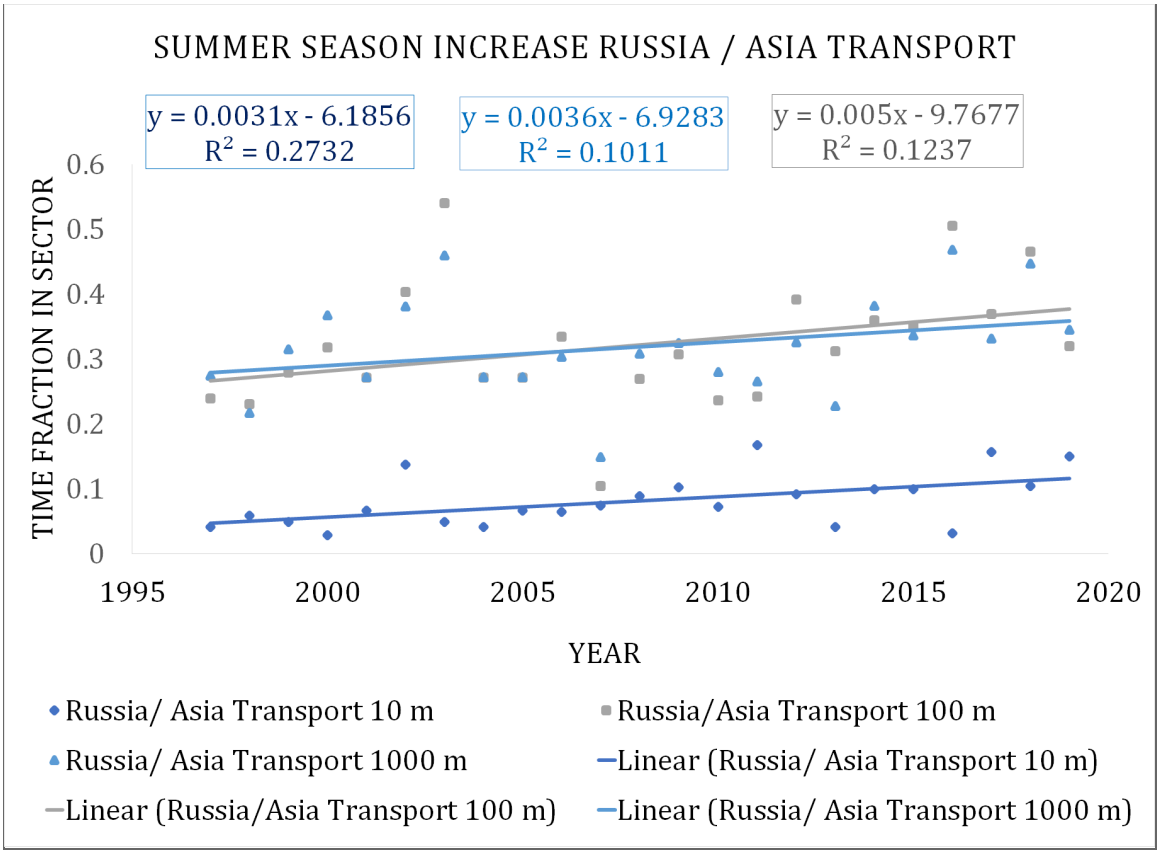

Sector, Season, and Arrival Height	Significance	Sen's Slope	R^2	% change
Russia/Asia Summer at 10m	95%	0.006	0.27	1.8%
Russia/Asia Summer at 100m	95%	0.005	0.12	1.6%
Russia/Asia Summer at 1000m	90%	0.004	0.10	1.1%

Figure 20: Summer transport from the Russia / Asia sector shows significant increases for all three arrival heights. R^2 values are 0.27 for 10m, 0.10 for 100m, and 0.12 for 1000m. Sen's slope estimates suggest a positive association from Russia / Asia transport over time.

3.3 Trends in Optical Properties at Utqiaġvik, Alaska

Aerosols affect the Earth's radiation budget in two ways: 1) direct forcing due to absorption and scattering of incoming solar radiation 2) through cloud nucleation processes and subsequent changes to cloud microphysical (cloud drop number concentration and size) and macrophysical (extent, lifetime) properties (Boucher et al. 2013, IPCC 2013, Yin and Min 2014). In fact, this interaction is the greatest source of uncertainty in climate modeling (IPCC 2013). The urgency of understanding the connection between these phenomena is compounded in the Arctic since influxes of solar radiation enhance the ice-albedo positive feedback that drives Arctic amplification (Quinn et al. 2008). Therefore, determining and quantifying the effect that atmospheric chemical composition has on radiative forcing in the Arctic is imperative.

The sawtooth patterns observed with the nss $SO_4^=$ and NO_3^- measurements in figure 7 are echoed by annual aerosol scattering and absorption measurements, though this data set extends from 1998 to 2019 (figures 21 and 22). These patterns correspond with seasonal aerosol loading and accumulation and demonstrate how chemical composition of the atmosphere affects aerosol optical properties. As noted in sections 3.1 and 3.2, winter emission reductions in North America and Europe seem to have resulted in significant haze season absorption and scattering decreases (figure 23). Haze season scattering at 550 nm is also decreasing for submicron particles (-1.9% decrease, 99% significance). The strong decreasing trends in nss $SO_4^=$ likely explain the decrease in aerosol scattering at Utqiaġvik (figures 3 and 8).

In addition to decreases in submicron scattering at 550 nm in the haze season, submicron aerosol absorption at 550 nm is also decreasing (-2.62% decrease, 99% significance). Though the cause of the absorption decrease in this study remains speculative, it is most likely that it is tied to black carbon emissions since it is the most efficient absorbing aerosol species. Black carbon, though a minor component of Arctic haze, is a major contributor to aerosol radiative effects through direct forcing and deposition on snow and ice which leads to darker exposed surfaces (IPCC 2013, Shen 2017). Haze season black carbon is anthropogenically produced at lower latitudes via fossil fuel combustion and biomass burning and then carried to the Arctic with more efficient wintertime transport (IPCC 2013, Shen et al. 2017). Decreased industrial and fossil fuel emissions from Europe and North America have not only resulted in less SO_2 but also less black carbon (Ren et al. 2020). Europe is considered a major source region for Arctic black carbon, so emission reductions over the last several decades may explain the simultaneous decrease in absorption and scattering at Utqiaġvik (AMAP 2006, Stohl 2006, Shen et al. 2017, Ren et al. 2020).

Summer trends in aerosol optical properties at Utqiaġvik may be associated with biogenic nss sulfate production, but only to a minor extent. Current analysis in this study signifies that supermicron scattering at 550 nm may be increasing in the summer, however, there is not enough data to demonstrate statistical significance yet (figures 3 and 24). Sea salt aerosol makes up a significant portion of particle mass in the summer and contributes significantly to aerosol scattering. The increase in scattering in this study, however, is not related to supermicron sodium and

chloride aerosol since the current analysis suggests decreasing concentrations for these two species by -4.05% and -5.6% respectively (figures 11 and 24). While the main driver of this trend is unknown at this time, the increase in supermicron scattering may be partially due to increased concentrations of supermicron nss $SO_4^=$. Nonetheless, since summertime concentrations of nss $SO_4^=$ are still relatively low compared to other species in the summer, it is unlikely that it is the main cause for increased supermicron scattering (Quinn et al. 2002).

Aerosol fine fraction scattering is also decreasing in the summer (-3.8% decrease, 99% significance) (figure 25). Fine fraction is the ratio of submicron to sub-10 micron scattering, and therefore a decrease in fine fraction scattering could be tied to decreased submicron scattering species or increased supermicron scattering species. For this trend, sea salt aerosol concentrations would also be an intuitive influencing factor since sea salt dominates supermicron aerosol particle mass and scattering, and is projected to increase in the next several decades with climate change (Struthers et al. 2011). Data in this study does not support this theory since supermicron sodium and chloride concentrations seem to be decreasing as submicron concentrations are increasing (figure 11). Both of these trends would increase fine fraction scattering, so the primary production of sea salt aerosol is unlikely to be the reason for a significant decrease in fine fraction scattering. As mentioned before, nss $SO_4^=$ is a minor component of aerosol mass in the summer, and increased concentrations do not necessarily explain the decrease in fine fraction scattering. Thus, the reason fine fraction scattering is decreasing is currently an open question.

The summer increase in supermicron absorption at 550 nm (+4.4% increase, 99% significance) in figure 24 is likely tied to black and organic carbon, which exhibit strong absorption properties (Stohl 2006, Stohl et al. 2007, Quinn et al. 2008, Shen et al. 2017). This long-term increase in supermicron absorption suggests that increased frequency and duration of summertime boreal fire activity, agricultural burning, diesel combustion, or a combination of these factors could affect aerosol composition in the Arctic (IPCC 2013, Shen et al. 2017, Stohl et al. 2006, Stohl et al. 2007, Quinn et al. 2008). Because supermicron particles exhibit shorter atmospheric lifetimes, source regions for the transport of absorbing species are confined to the northernmost latitudes of North America, Europe, and Russia/Asia and within the Arctic (Stohl et al. 2006, Quinn et al. 2008). An inconsistency in the summer supermicron absorption measurements should be noted for the haze season and summer seasons of 2016, which is shown in figure 22. The 2016 haze season had an uncharacteristically low absorption coefficient while the summer season coefficient was uncharacteristically high (figure 22). Analysis of the data from that year did not reveal any outstanding influential values or measurement errors, so an explanation for this discrepancy in the time series is not apparent at this time.

Summertime processes for aerosol formation, especially primary production of sea salt aerosol and biogenic nss sulfate, enhance aerosol scattering and cloud albedo effects. The increase in summertime supermicron scattering and nss $SO_4^=$ aerosol in this study agrees with findings from Yin and Min (2014) on cloud properties and radiative forcing at Utqiaġvik (Yin and Min 2014). Yin and Min (2014) compared the net radiative forcings for the winter and summer seasons at

Utqiaġvik from 1998 to 2012, which showed that the surface temperature warming rate between 1998-2012 in the haze season was 41% stronger than in the summer (Yin and Min 2014). The study attributed accelerated surface warming in the haze season to ice cloud formation and decreased cloud optical depth (COD), water vapor path (WVP), and liquid water path (LWP). COD, WVP, and LWP were all statistically correlated with wintertime surface temperatures and consistent with positive cloud radiation feedback (Yin and Min 2014). In the summer, Yin and Min (2014) found that clouds have a cooling effect on net surface radiation and surface temperatures with reduced WVP, but increased LWP and cloud amount (Yin and Min 2014). They attributed the enhanced cloud cooling properties to summertime biogenic aerosol production and dominance of liquid-water clouds over ice clouds (Yin and Min 2014). Both of these processes reduce surface heating in the summer and combat accelerated warming in the Arctic (Yin and Min 2014). The results from this study and Yin and Min (2014) suggest that summertime aerosol processes are likely inducing a cooling effect on Arctic radiative forcing, though more modeling is needed to confirm a direct relationship between atmospheric chemistry and radiative properties at Utqiaġvik (Yin and Min 2014).

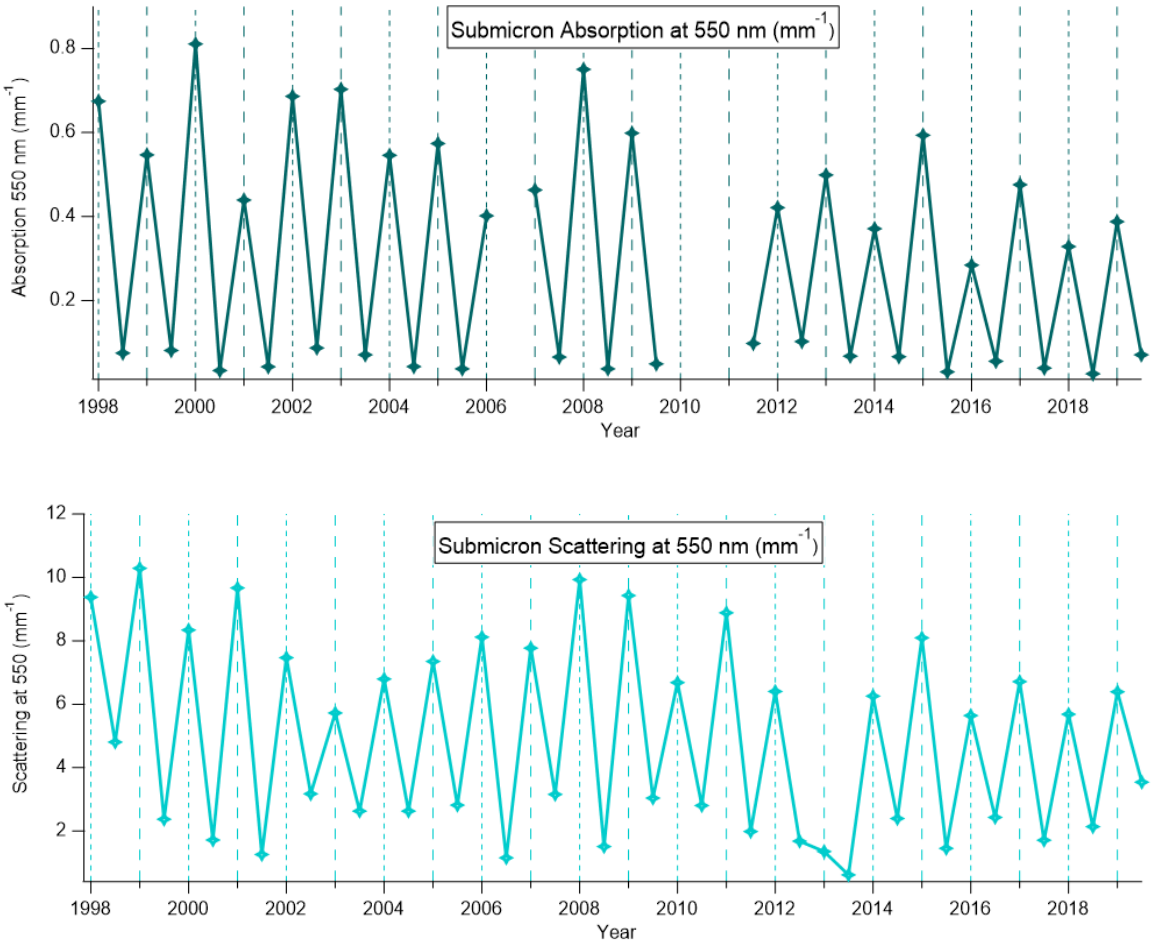

Figure 21: Absorption and scattering for submicron particles at 550 nm. The upper time series shows seasonal averages for submicron absorption and the bottom time series shows seasonal averages for submicron scattering.

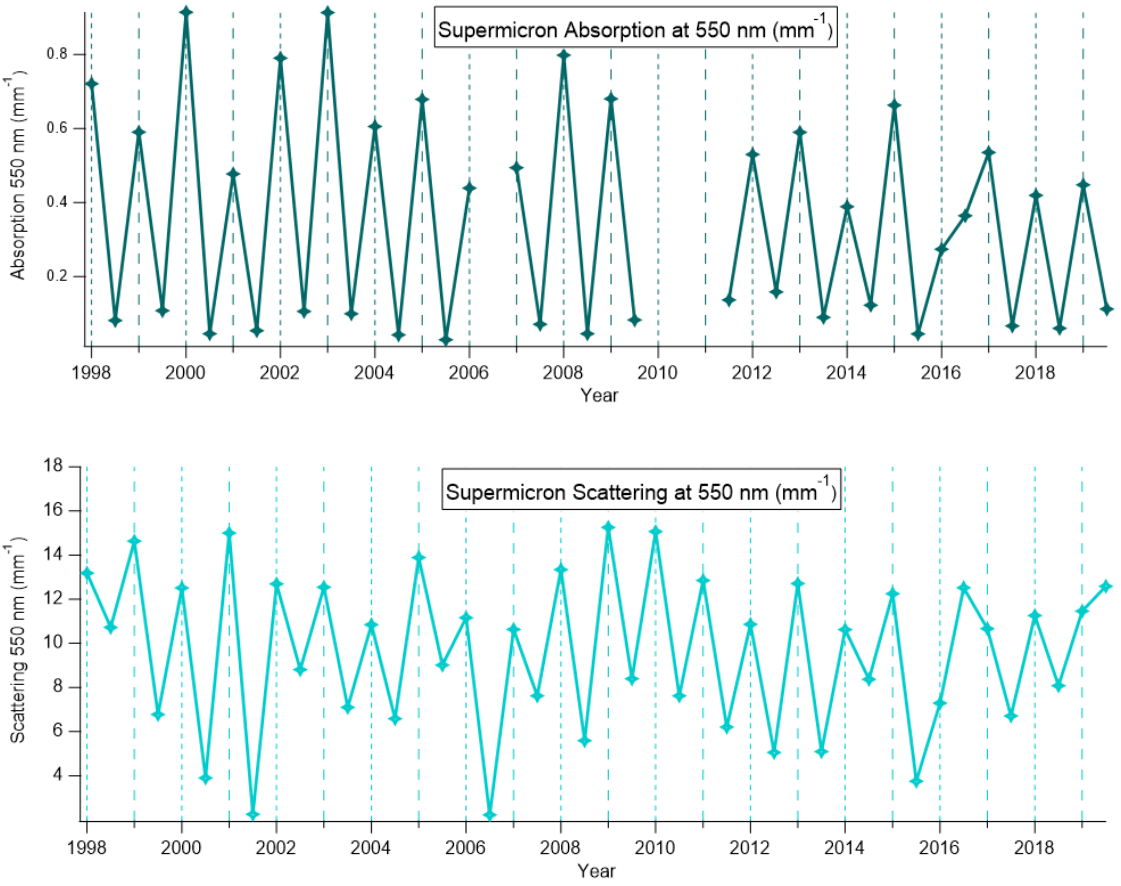

Figure 22: Absorption and scattering for supermicron particles at 550 nm. The upper time series shows seasonal averages for supermicron absorption and the bottom time series shows seasonal averages for supermicron scattering.

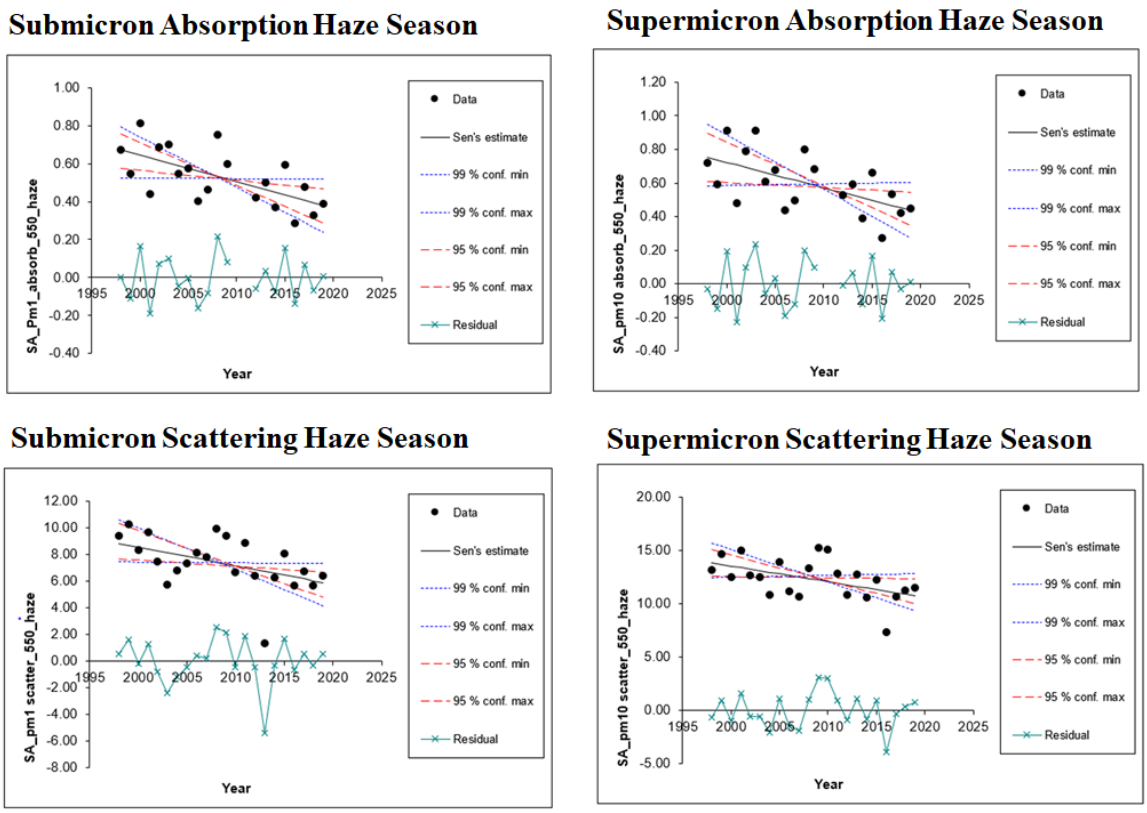

Trends in Absorption and Scattering at 550 nm in Haze Season (1998-2019)				
Parameter	Particle Size	Significance	Sen's Slope	% change
Absorption at 550 nm	Submicron	99%	-0.014	-2.6
Absorption at 550 nm	Supermicron		-0.001	-1.3
Scattering at 550 nm	Submicron	99%	-0.140	-1.9
Scattering at 550 nm	Supermicron		0.007	0.15

Figure 23: MAKESENS trends for absorption and scattering in the haze season. Submicron (left) and supermicron (right) absorption are above with submicron (left) and supermicron (right) scattering below.

Submicron Absorption Summer Season

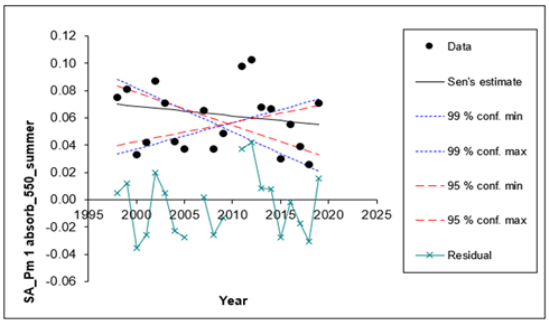

Supermicron Absorption Summer Season

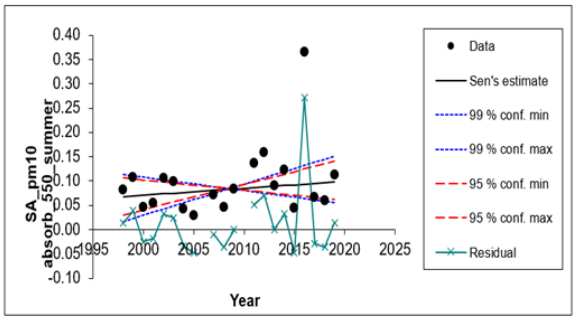

Submicron Scattering Summer Season

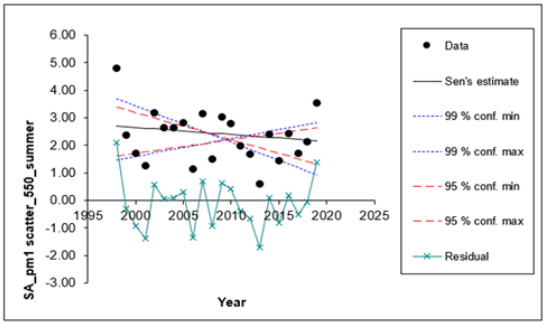

Supermicron Scattering Summer Season

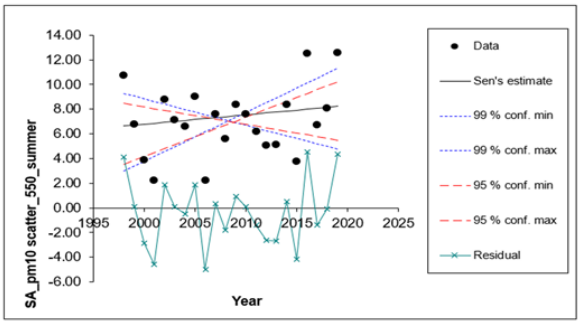

Trends in Absorption and Scattering at 550 nm in Summer Season (1998-2019)				
Parameter	**Particle Size**	**Significance**	**Sen's Slope**	**% change**
Absorption at 550 nm	Submicron	-	-0.001	-1.2
Absorption at 550 nm	Supermicron	99%	0.002	4.4
Scattering at 550 nm	Submicron	-	-0.026	-1.1
Scattering at 550 nm	Supermicron	-	0.098	2.1

Figure 24: MAKESENS trends for Absorption and scattering in the summer season. Submicron (left) and supermicron (right) Absorption are above with submicron (left) and supermicron (right) scattering below.

Fine Fraction in Haze Season

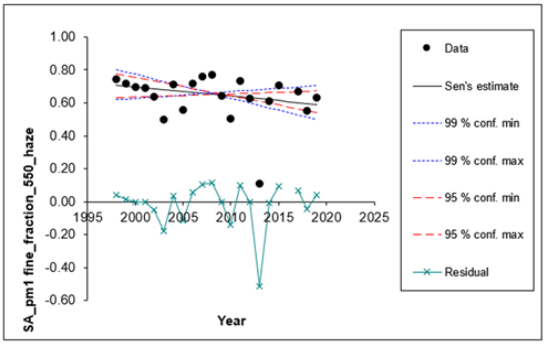

Fine Fraction in Summer Season

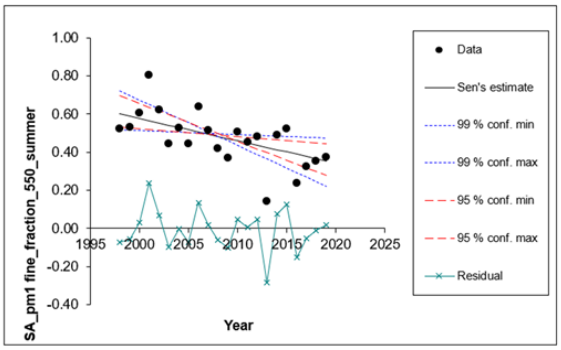

Trends in Fine Fraction at 550 nm in Summer Season (1998-2019)				
Parameter	**Particle Size**	**Significance**	**Sen's Slope**	**% change**
Haze Season	Submicron/ sub-10 micron	-	-0.034	-1.9
Summer Season	Submicron/ sub-10 micron	99%	-0.022	-3.9

Figure 25: Fine fraction scattering for submicron particles in haze (left) and summer (right) seasons. There is a 99% significant decreasing trend for summer submicron particles.

VI. Conclusion

Findings from this study highlight some key changes in aerosol sources, composition, and optical properties at Utqiaġvik. Notably, there have been significant decreases in nss $SO_4^=$ and NO_3^- concentrations in the haze season from 1998 to 2013. Nss $SO_4^=$ concentrations decreased by -2.9% for submicron particles (p-value<0.1) and -12% for supermicron particles (p-value<0.01) while supermicron NO_3^- decreased by -8.2% (p-value <0.01). These trends occur simultaneously with the decrease in haze season transport from the Europe sector by -2.0% at 10m (p-value<0.05) and -1.7% at 100m (p-value<0.05) and emission reductions in Europe and North America from 1997-2020 (Klimont et al. 2012, Tørseth et al. 2012, Hidy et al. 2016). Consequently, there has been a significant decrease in haze season scattering for submicron particles by -2.6% observed between 1998-2019 (p-value<0.01).

Since non-sea salt sulfate and nitrate aerosol scatter incoming solar radiation, decreased concentrations may have a net warming effect on the Arctic atmosphere (IPCC 2013). Haze season warming at Utqiaġvik is also related to cloud formation processes. Yin and Min (2014) analyzed aerosol and cloud optical properties at Utqiaġvik between 1998 to 2012, and revealed haze season decreases in cloud liquid water path and optical depths that showed positive correlations with surface temperature (Yin and Min 2014). These results suggested that positive cloud radiation feedback is occurring and enhancing surface warming in the haze season (Yin and Min 2014). Observations of a decreasing trend in aerosol scattering in this study in conjunction with Yin and Min's findings suggest that changes in aerosol and

cloud composition at Utqiaġvik could induce a net warming effect in the haze season (IPCC 2013, Yin and Min 2014). Increased Arctic surface temperatures propagate to cause earlier onset of springtime ice melt and increases the duration of non-snow cover on the Arctic surface (Yin and Min 2014). Thus, positive cloud-radiation feedback and ice-albedo feedback processes are intertwined and synergistically contribute to accelerated wintertime and springtime warming.

Aerosol acidity is decreasing as more nss sulfate and nitrate particles are being neutralized by ammonium aerosol. The results of this study demonstrate a moderate correlation between nss $SO_4^=$ and NH_4^+ ratios with weaker correlation in the haze season (R^2=0.42, p-value<0.001) compared to the summer season (R^2=0.56, p-value<0.001). Since ammonium sulfate formation has important implications for direct scattering, hygroscopic properties of aerosols, and cloud nucleation processes, additional work analyzing the partitioning of these three species is merited (Fisher et al. 2011, IPCC 2013).

Haze season aerosol composition appears to be becoming increasingly neutralized based on concentrations of nss sulfate and nitrate alone. Additionally, in the same season, acid-derived chloride depletion does not seem to be as prevalent as originally anticipated. Prior literature emphasizes the important role nitrate and sulfate aerosols play in chloride depletion, and the relative increase of aerosol acidity in the haze season at Utqiaġvik should theoretically result in some degree of chloride depletion (Yao et al. 2003, Zao and Gao 2008). The expected separation between the measured submicron Cl^-:Na^+ molar ratio and the ratio in seawater was not observed in figure 12, so results from this study indicate that submicron

chloride depletion is not directly observable, despite enhanced seasonal nss sulfate and nitrate concentrations. The lack of visible chloride depletion in the haze season submicron Cl^-:Na^+ linear regression may be an early indicator that decreased aerosol acidity could impact pH-driven reactions on sea salt particles.

Besides the decrease in acidic species, another cause for the lack of submicron haze season chloride depletion could be the significant increase in transport from the ocean-dominated Pacific sector during this time. The increase in haze season Pacific transport is one of the more enigmatic results of this study, as correlation with atmospheric and oceanic oscillation data was nonexistent. The enhanced transport could be due to the weakening of the Arctic front and more favorable transport pathways becoming available (Stohl 2006, AMAP 2008, Quinn et al. 2008, Fisher et al. 2011), but this theory cannot be confirmed through this study.

Increased summer supermicron nss $SO_4^=$ concentrations (+9.7%, p-value>0.1) and supermicron scattering (+4.4% p-value<0.01), and decreased fine fraction scattering (-3.8%, p-value<0.01) suggest that local summertime aerosol formation processes could be changing in the Arctic; however, these results are not necessarily connected. The time-scale of this study was not long enough to detect statistically significant increases in summertime supermicron biogenic sulfate, chloride, or sodium. In fact, decreased supermicron sodium and chloride concentrations directly oppose expected consequences of increased Arctic SSTs, reduced sea ice extent, and longer melt seasons (May et al. 2016, Struthers et al. 2011). These climatological factors are also expected to enhance biogenic sulfate formation, which current trend analysis for supermicron nss $SO_4^=$ concentrations

seems to support (Quinn et al. 2002, Quinn et al. 2008, Sharma et al. 2012, Wang et al. 2018).

Summertime trends in this study are more confounding since the data do not provide clear explanations for the observed increase in supermicron scattering and decrease in fine fraction scattering. Additionally, causes for the increase in supermicron aerosol absorption remain speculative since direct case studies are needed to tie this trend to biomass burning events empirically. Expansion of this analysis to the present time may help resolve some of the ambiguity regarding summertime aerosol processes at Utqiaġvik.

The Arctic is warming two to four times faster than the rest of the planet and is among the most vulnerable regions to climate change, which is why understanding ties between aerosols, radiative forcing, and climatological feedback processes is imperative for mitigating the impacts of global warming in the coming decades (AMAP 2008, IPCC 2013, Ren et al. 2020). It is evident that the relationships between pollution, aerosol formation, and climate forcing are complex; in this long-term data set, pollution reductions seemed to have a net warming effect in the Arctic in the haze season. Conversely, enhanced local aerosol formation processes may be inducing a cooling effect in the summer. Climatological phenomena including the rise in sea surface temperatures, reduced sea ice cover, and weakening of the Arctic front grow increasingly concerning with every anomalous year we observe on record (IPCC 2013). Since aerosol and cloud radiative properties are among the greatest uncertainties in climate modeling, progress in this field, especially in the fastest-changing regions, contributes to our

goal to understand and mitigate the causes of climate change. To address this need, continued long-term observations of chemical composition and optical properties at Utqiaġvik are needed.

V. References

AMAP Assessment 2006: Acidifying Pollutants, Arctic Haze, and Acidification in the Arctic. *Arctic Monitoring and Assessment Programme (AMAP)*, Oslo, Norway. xii + 112pp. https://oaarchive.arctic-council.org/handle/11374/705

Abbatt, J. P., 2006: Solid Ammonium Sulfate Aerosols as Ice Nuclei: A Pathway for Cirrus Cloud Formation. *Science*, **313**, 1770–1773, doi:10.1126/science.1129726.

Barrie, L. A., and R. M. Hoff, 1984: The oxidation rate and residence time of sulphur dioxide in the arctic atmosphere. *Atmospheric Environment (1967)*, **18**, 2711–2722, doi:10.1016/0004-6981(84)90337-8.

Berner, A., Lürzer, C., Pohl, F., Preining, O., and Wagner, P., 1979: The size distribution of the urban aerosol in Vienna. *Science of The Total Environment*, **13(3)**, 245–261. doi:10.1016/0048-9697(79)90105-0

Bond, T. C., Anderson, T. L., and Campbell, D., 1999: Calibration and Intercomparison of Filter-Based Measurements of Visible Light Absorption by Aerosols. *Aerosol Science and Technology*, **30(6)**, 582–600. doi:10.1080/027868299304435

Boucher, O., et al., 2013: Clouds and aerosols, in Climate Change 2013: The Physical Science Basis. *Contribution of Working Group I to the Fifth Assessment Report of the Intergovernmental Panel on Climate Change,* edited by T. F. Stocker et al., pp. 571–658, Cambridge Univ. Press, Cambridge, U. K., and New York.

Bauer, S. E., D. Koch, N. Unger, S. M. Metzger, D. T. Shindell, and D. G. Streets, 2007: Nitrate aerosols today and in 2030: a global simulation including aerosols and tropospheric ozone. *Atmospheric Chemistry and Physics*, **7,** 5043–5059, doi:10.5194/acp-7-5043-2007.

Daubrée, M., 1874: D'observations faites par M. le profes-seur Nordenskiöld. *Comptes Rendus*, **78**, 236–239.

Delene, D. J., and J. A. Ogren, 2002: Variability of Aerosol Optical Properties at Four North American Surface Monitoring Sites. *Journal of the Atmospheric Sciences*, **59**, 1135–1150, doi:10.1175/1520-0469(2002)059<1135:voaopa>2.0.co;2.

Dennis, R. L., Bhave, P. V., andamp; Pinder, R. W., 2008: Observable indicators of the sensitivity of PM2.5 nitrate to emission reductions—Part II: Sensitivity to errors in total ammonia and total nitrate of the CMAQ-predicted non-linear effect of SO2 emission reductions. *Atmospheric Environment*, **42(6)**, 1287–1300. doi:10.1016/j.atmosenv.2007.10.036

Feng, L., H. Shen, Y. Zhu, H. Gao, and X. Yao, 2017: Insight into Generation and Evolution of Sea-Salt Aerosols from Field Measurements in Diversified Marine and Coastal Atmospheres. *Scientific Reports*, **7**, doi:10.1038/srep41260.

Ferek, R. J., P. V. Hobbs, L. F. Radke, J. A. Herring, W. T. Sturges, and G. F. Cota, 1995: Dimethyl sulfide in the Arctic atmosphere. *Journal of Geophysical Research*, **100**, 26093, doi:10.1029/95jd02374.

Fisher, J. A., and Coauthors, 2011: Sources, distribution, and acidity of sulfate–ammonium aerosol in the Arctic in winter–spring. *Atmospheric Environment*, **45**, 7301–7318, doi:10.1016/j.atmosenv.2011.08.030.

Gettelman, A., X. Liu, D. Barahona, U. Lohmann, and C. Chen, 2012: Climate impacts of ice nucleation. *Journal of Geophysical Research: Atmospheres*, 117, doi:10.1029/2012jd017950.

Guo, H., Sullivan, A. P., Campuzano-Jost, P., Schroder, J. C., Lopez-Hilfiker, F. D., Dibb, J. E., et al., 2016: Fine particle pH and the partitioning of nitric acid during winter in the northeastern United States. *Journal of Geophysical Research: Atmospheres*, **121(17)**. doi:10.1002/2016jd025311

Hand, J. L., and W. C. Malm, 2007: Review of aerosol mass scattering efficiencies from ground-based measurements since 1990. *Journal of Geophysical Research*, **112**, doi:10.1029/2007jd008484.

Hara, K., Osada, K., Hayashi, M., Matsunaga, K., Shibata, T., Iwasaka, Y., and amp; Furuya, K., 1999: Fractionation of inorganic nitrates in winter Arctic troposphere: Coarse aerosol particles containing inorganic nitrates. Journal of Geophysical Research: Atmospheres, **104(D19)**, 23671–23679. doi:10.1029/1999jd900348

Hara, K., K. Osada, K. Matsunaga, Y. Iwasaka, T. Shibata, and K. Furuya, 2002): Atmospheric inorganic chlorine and bromine species in Arctic boundary layer of the winter/spring, *J. Geophys. Res.*, **107(D18)**, 4361, doi:10.1029/2001JD001008.

Hara, K., K. Osada, M. Kido, K. Matsunaga, Y. Iwasaka, G. Hashida, and T. Yamanouchi, 2005: Variations of constituents of individual sea-salt particles at Syowa station, Antarctica. Tellus B: Chemical and Physical Meteorology, **57**, 230–246, doi:10.3402/tellusb.v57i3.16530.

Hess, G. D. ,1998: An Overview of the HYSPLIT_4 Modelling System for Trajectories, Dispersion, and Deposition. Silver Spring, Maryland, U.S.A.: NOAA Air Resources Laboratory.

Hidy, G. M., C. L. Blanchard, D. Helmig, and D. Liptzin, 2016: The changing face of lower tropospheric sulfur oxides in the United StatesLower troposphere sulfur oxides. *University of California Press*. https://online.ucpress.edu/elementa/article/doi/10.12952/journal.elementa.0001

38/112878/The-changing-face-of-lower-tropospheric-sulfur (Accessed March 14, 2021).

Jacobi, H. W., D. Voisin, J. L. Jaffrezo, J. Cozic, and T. A. Douglas, 2012: Chemical composition of the snowpack during the OASIS spring campaign 2009 at Barrow, Alaska, *J. Geophys. Res.*, **117**, D00R13, doi:10.1029/2011JD016654.

Klimont, Z., S. J. Smith, and J. Cofala, 2013: The last decade of global anthropogenic sulfur dioxide: 2000–2011 emissions. *Environmental Research Letters*, **8**, 014003, doi:10.1088/1748-9326/8/1/014003.

Law, K. S., and A. Stohl, 2007: Arctic Air Pollution: Origins and Impacts. Science, **315**, 1537–1540, doi:10.1126/science.1137695.

Law, K. S., and Coauthors, 2014: Arctic Air Pollution: New Insights from POLARCAT-IPY. *Bulletin of the American Meteorological Society*, **95**, 1873–1895, doi:10.1175/bams-d-13-00017.1.

Mantua, N. J., and S. R. Hare, 2002: The Pacific Decadal Oscillation. Journal of Oceanography, **58**, 35–44, doi:10.1023/a:1015820616384.

May, N. W., Quinn, P. K., McNamara, S. M., and Pratt, K. A., 2016: Multiyear study of the dependence of sea salt aerosol on wind speed and sea ice conditions in the coastal Arctic. *Journal of Geophysical Research: Atmospheres*, **121(15)**, 9208–9219. doi:10.1002/2016jd025273

McInnes, L. M., D. S. Covert, P. K. Quinn, and M. S. Germani, 1994: Measurements of chloride depletion and sulfur enrichment in individual sea-salt particles collected from the remote marine boundary layer. *Journal of Geophysical Research*, **99**, 8257, doi:10.1029/93jd03453.

Quinn, P. K., V. N. Kapustin, T. S. Bates, and D. S. Covert, 1996: Chemical and optical properties of marine boundary layer aerosol particles of the mid-Pacific in relation to sources and meteorological transport. Journal of Geophysical Research: Atmospheres, 101, 6931–6951, doi:10.1029/95jd03444.

Quinn, P. K., Miller, T. L., Bates, T. S., Ogren, J. A., Andrews, E., and Shaw, G. E., 2002: A 3-year record of simultaneously measured aerosol chemical and optical properties at Barrow, Alaska. *Journal of Geophysical Research: Atmospheres*, **107(D11)**. doi:10.1029/2001jd001248

Quinn, P. K., Shaw, G., Andrews, E., Dutton, E. G., Ruoho-Airola, T., and Gong, S. L., 2007: Arctic haze: current trends and knowledge gaps. *Tellus B*, **59(1)**. doi:10.3402/tellusb.v59i1.16972

Quinn, P. K., Bates, T. S., Bond, T., Burkhart, J. F., Fiore, A. M., Flanner, M., et al., 2008: The Impact of Short-Lived Pollutants on Arctic Climate. Oslo: Arctic Monitoring and Assessment Programme (AMAP).

Quinn, P. K., Bates, T. S., Baum, E., Doubleday, N., Fiore, A. M., Flanner, M., et al., 2008: Short-lived pollutants in the Arctic: their climate impact and possible mitigation strategies. *Atmospheric Chemistry and Physics*, **8(6)**, 1723–1735. doi:10.5194/acp-8-1723-2008

Quinn, P. K., Bates, T. S., Schulz, K., and Shaw, G. E., 2009: Decadal trends in aerosol chemical composition at Barrow, Alaska: 1976–2008. *Atmospheric Chemistry and Physics*, **9(22)**, 8883–8888. doi:10.5194/acp-9-8883-2009

Ren, L., Y. Yang, H. Wang, R. Zhang, P. Wang, and H. Liao, 2020: Source attribution of Arctic black carbon and sulfate aerosols and associated Arctic surface warming during 1980–2018. *Atmospheric Chemistry and Physics*, **20**, 9067–9085, doi:10.5194/acp-20-9067-2020.

Salmi, T., 2002: *Detecting trends of annual values of atmospheric pollutants by the Mann-Kendall test and Sen's slope estimates: the Excel template application MAKESENS*. Helsinki: Finnish Meteorological Institute.

Schlosser, J. S., Braun, R. A., Bradley, T., Dadashazar, H., MacDonald, A. B., Aldhaif, A. A., et al., 2017: Analysis of aerosol composition data for western United States wildfires between 2005 and 2015: Dust emissions, chloride depletion, and most enhanced aerosol constituents. *Journal of Geophysical Research: Atmospheres*, **122(16)**, 8951–8966. doi:10.1002/2017jd026547

Schneider, N., and B. D. Cornuelle, 2005: The Forcing of the Pacific Decadal Oscillation*. *Journal of Climate*, **18**, 4355–4373, doi:10.1175/jcli3527.1.

Sharma, S., Chan, E., Ishizawa, M., Toom-Sauntry, D., Gong, S. L., Li, S. M., et al., 2012: Influence of transport and ocean ice extent on biogenic aerosol sulfur in the Arctic atmosphere. *Journal of Geophysical Research: Atmospheres*, **117(D12)**. doi:10.1029/2011jd017074

Shaw, G. E., 1982: Evidence for a central Eurasian source area of Arctic haze in Alaska. Nature, **299**, 815–818.

Shaw, G. E., 1982: Sources of transport of Arctic pollution aerosol: A chronicle of six years of ONR research. Naval Res. Rev., **34**, 3–27.

Shaw, G. E., 1995: The Arctic Haze Phenomenon. Bulletin of the American Meteorological Society, **76**, 2403–2413, doi:10.1175/1520-0477(1995)076<2403:tahp>2.0.co;2.

Shen, Z., Ming, Y., Horowitz, L. W., Ramaswamy, V., and Lin, M., 2017: On the Seasonality of Arctic Black Carbon. *Journal of Climate*, **30(12)**, 4429–4441. doi:10.1175/jcli-d-16-0580.1

Stohl, A., Andrews, E., Burkhart, J. F., Forster, C., Herber, A., Hoch, S. W., et al., 2006: Pan-Arctic enhancements of light-absorbing aerosol concentrations due to North American boreal forest fires during summer 2004. *Journal of Geophysical Research*, **111(D22)**. doi:10.1029/2006jd007216

Stohl, A., Berg, T., Burkhart, J. F., Fjæraa, A. M., Forster, C., Herber, A., et al., 2007: Arctic smoke – record-high air pollution levels in the European Arctic due to agricultural fires in Eastern Europe in spring 2006. *Atmospheric Chemistry and Physics*, **7(2),** 511–534. doi:10.5194/acp-7-511-2007

Stone, R. S., Sharma, S., Herber, A., Eleftheriadis, K., and Nelson, D. W., 2014: A characterization of Arctic aerosols on the basis of aerosol optical depth and black carbon measurements. *Elementa: Science of the Anthropocene*, **2**. doi:10.12952/journal.elementa.000027

Struthers, H., A. M. Ekman, P. Glantz, T. Iversen, A. Kirkevåg, E. M. Mårtensson, Ø. Seland, and E. D. Nilsson, 2011: The effect of sea ice loss on sea salt aerosol concentrations and the radiative balance in the Arctic. *Atmospheric Chemistry and Physics*, **11**, 3459–3477, doi:10.5194/acp-11-3459-2011.

Taylor, C. J., 1981: First International Polar Year, 1882-83. *ARCTIC*, **34**, doi:10.14430/arctic2540.

Tomasi, C., and Coauthors, 2007: Aerosols in polar regions: A historical overview based on optical depth and in situ observations. *Journal of Geophysical Research*, **112**, doi:10.1029/2007jd008432.

Tørseth, K., and Coauthors, 2012: Introduction to the European Monitoring and Evaluation Programme (EMEP) and observed atmospheric composition change during 1972–2009. *Atmospheric Chemistry and Physics*, **12**, 5447–5481, doi:10.5194/acp-12-5447-2012.

Wang, S., M. Maltrud, S. Elliott, P. Cameron-Smith, and A. Jonko, 2018: Influence of dimethyl sulfide on the carbon cycle and biological production. *Biogeochemistry*, **138**, 49–68, doi:10.1007/s10533-018-0430-5.

Yin, B., and Min, Q., 2014: Climatology of aerosol and cloud optical properties at the Atmospheric Radiation Measurements Climate Research Facility Barrow and Atqasuk sites. *Journal of Geophysical Research: Atmospheres*, **119(4)**, 1820–1834. doi:10.1002/2013jd020296

Zhao, B., and Coauthors, 2019: Ice nucleation by aerosols from anthropogenic pollution. Nature Geoscience, **12**, 602–607, doi:10.1038/s41561-019-0389-4.

Zhao, Y., and Y. Gao, 2008: Acidic species and chloride depletion in coarse aerosol particles in the US east coast. *Science of The Total Environment*, **407**, 541–547, doi:10.1016/j.scitotenv.2008.09.002.